6-Methoxy-*N*-alkyl Isatin Acylhydrazone Derivatives as a Novel Series of Potent Selective Cannabinoid Receptor 2 Inverse Agonists: Design, Synthesis, and Binding Mode Prediction

Philippe Diaz,[†] Sharangdhar S. Phatak,[‡] Jijun Xu,[†] Fanny Astruc-Diaz,[†] Claudio N. Cavasotto,[‡] and Mohamed Naguib*[,†]

Department of Anesthesiology and Pain Medicine, Unit 409, The University of Texas M. D. Anderson Cancer Center, 1400 Holcombe Boulevard, Houston, Texas 77030, School of Health Information Sciences, The University of Texas Health Science Center at Houston, 7000 Fannin, Suite 860B, Houston, Texas 77030

Received October 27, 2008

Recently, we discovered and reported a series of *N*-alkyl isatin acylhydrazone derivatives that are potent CB2 agonists. Here, we describe a novel series of selective CB2 inverse agonists resulting from introduction of a methoxy moiety in position 6 of the isatin scaffold. These novel 6-methoxy-*N*-alkyl isatin acylhydrazone derivatives exhibited high CB2 functional activity and selectivity at human CB2. Compound **16** (MDA77) had high activity (EC_{50} = 5.82 nM) at CB2 and no activity at CB1. Compound **15** (MDA55) (K_i = 89.9 nM, EC_{50} = 88.2 nM at CB2) inhibited the effect of compound **1** (MDA7), a selective CB2 agonist, in an animal model of neuropathic pain. The molecular modeling study presented here represents a first study of CB2 based on the structure of β_2-adrenergic receptor. A ligand-based homology model of the CB2 binding site was developed, and on the basis of our results, we propose a general binding mode for this class of inverse agonists with CB2.

Introduction

The endogenous cannabinoid (endocannabinoid) system consists of cannabinoid receptors (cannabinoid receptor 1 [CB1][a] and cannabinoid receptor 2 [CB2]), endogenous ligands, and several proteins responsible for their synthesis, transport, and hydrolysis. In animal models of allergic contact dermatitis[1] and peripheral neuropathy,[2] increases in endocannabinoid levels seem to represent a protective mechanism aimed at counteracting pain and inflammation.[3] The two cannabinoid receptors, CB1 and CB2, have been characterized and cloned.[4,5]

CB1 is found predominantly in the brain, where the highest densities are in the hippocampus, cerebellum, and striatum.[6] Cognitive impairment (and psychoactivity) induced by Δ^9-tetrahydrocannabinol is mediated by CB1 in the isocortex and allocortex (i.e., hippocampus).[7]

CB2 is expressed mainly on immune tissues—the spleen, tonsils, monocytes, and B and T lymphocytes.[5,8] Selective CB2 agonists appear to be devoid of central effects attributable to CB1 activation.[9,10] CB2 mRNA and/or proteins are increased during different inflammatory conditions. For example, it has been shown that CB2 expression is increased in the dorsal root ganglia and spinal cord of animals after spinal nerve ligation,[11,12] sciatic nerve injury,[13] or saphenous nerve ligation[14,15] in the bladder of rats after acute or chronic inflammation,[16] in women after endometrial inflammation,[17] and in humans and rats with acute pancreatitis.[18] CB_2 is up-regulated in reactive microglial cells in Alzheimer's disease, Huntington's disease, simian immunodeficiency virus-induced encephalitis, HIV encephalitis, and multiple sclerosis.[19−22] CB2 expression within immune cells, induction of CB2 expression after injury or inflammation, and the discovery that immunomodulation by cannabinoids is absent in CB2 knockout mice[23] suggest that CB2 plays a key role in immunomodulatory activity and have identified CB2 as an attractive therapeutic target for immunomodulation.[24−26]

Several CB2-selective inverse agonists have been described in the literature.[24]The chemical structures of a number of CB2 modulators are shown in Figure 1. Compound **3** is the first CB2-selective inverse agonist described.[27] As in the design of CB1 antagonists such as *N*-(piperidinyl)-5-(4-chlorophenyl)-1-(2,4-dichlorophenyl)-4-methyl-*1H*-pyrazole-3-carboxamide (SR141716), compound **3** was designed using a pyrazole moiety.[28] Compounds **2** and **3** have been extensively used as standards against which to measure the specificity of various cannabinoid agonists at CB2 in animal models. Half-maximal effective concentration (EC_{50}) values of compound **2** and compound **3** for inhibition of guanosine-5′-triphosphate (GTP)γ[^{35}S] binding to CB2 are 76.6 nM and 10.4 nM, respectively.[29]

Compound **6**, a CB2-selective inverse agonist, has been shown to inhibit carrageenin-induced mouse paw edema in a dose-dependent manner.[30] In addition, compound **6** inhibited immunoglobulin E-mediated cutaneous inflammation,[31] had antipruritic activity in a mouse model of chronic dermatitis,[32] and was also able to inhibit dinitrofluorobenzene- or 2-arachidonoylglycerol-induced ear swelling but had no effect on arachidonic acid-induced ear swelling.[33] On the other hand, in an animal model of cutaneous contact hypersensitivity, genetic deletion or pharmacologic blockade of cannabinoid receptors enhanced contact allergic inflammation.[1] The structure−activity relationships for some analogues of compound **6** have been described.[34]

Like compound **6**, compound **4** has been shown to be an immunomodulatory agent against inflammatory disorders in which leukocyte recruitment is involved.[25] The structure−activity relationships for this class of compounds have been described.[35] Compound **4** inhibited leukocyte trafficking induced by chemokines or by antigen challenge in several rodent in vivo models

* To whom correspondence should be addressed. Phone: 713-745-4948, Fax: 713-792-7591, E-mail: Naguib@mdanderson.org.

[†] Department of Anesthesiology and Pain Medicine, Unit 409, The University of Texas M. D. Anderson Cancer Center.

[‡] School of Health Information Sciences, The University of Texas Health Science Center at Houston.

[a] Abbreviations: CB1, cannabinoid receptor 1; CB2, cannabinoid receptor 2; DMSO, dimethyl sulfoxide; EC_{50}, half-maximal effective concentration; GTP, guanosine-5′-triphosphate; *h*CB1, human CB1; *h*CB2, human CB2; IC_{50}, median inhibition concentration; K_i, inhibition constant; NMR, nuclear magnetic resonance.

10.1021/jm801353p CCC: $40.75
Published on Web 12/30/2008

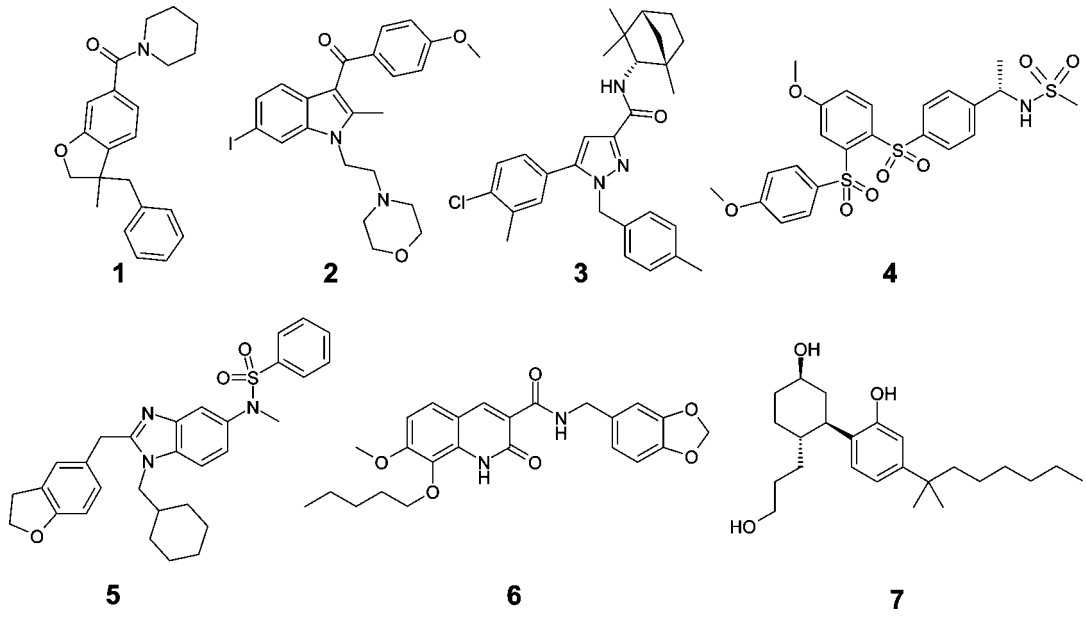

Figure 1. Chemical structures of CB2-selective modulators (**1**−**6**) and a nonselective CB agonist (**7**). (**1**) MDA7;[10] (**2**) AM630;[29] (**3**) SR144528;[27] (**4**) Sch.336;[36] (**5**) *N*-[1-cyclohexylmethyl-2-(2,3-dihydro-1-benzofuran-5-ylmethyl)-1*H*-benzimidazol-5-yl]-*N*-methylbenzenesulfonamide; (**6**) JTE-907;[30] (**7**) CP55,940.[77]

and blocked ovalbumin-induced lung eosinophilia in a mouse model of allergic asthma;[36] these effects have been attributed to down-regulation of phosphorylation of the monocyte-specific actin-binding protein L-plastin by compound **4**.[25] This mechanism may explain the ability of compound **4** to modulate immune cell mobility and explains its effects on antigen-induced monoarticular arthritis and autoimmune encephalomyelitis in the rat.

In a high-throughput screening program focused on CB2, a novel series of benzimidazole derivatives exhibiting CB2 affinity was recently identified.[37] After chemical optimization, compound **5** was described as a CB2 inverse agonist that showed a binding affinity for CB2 of 0.7 nM and an EC_{50} of 2.2 nM.[37] Compound **5** reversed the effect of a cannabinoid agonist in a competition assay with an inhibition constant (K_i) of 1.2 nM. In this series, the replacement of an ethoxyphenyl group with a benzofuran resulted in a change in biological activity from agonist to inverse agonist in functional assays.[37]

Recently, we described a novel series of CB2 agonists based on *N*-alkyl isatin acylhydrazone derivatives.[38] Similar to what was done by others for compound **5**, we sought to design and synthesize a novel series of CB2 inverse agonists by using our agonist scaffold and studying the impact of substitutions in the isatin ring on functional activity. Our first attempt, introducing electron-withdrawing or electron-donating groups in position 5 or 7 of the isatin ring, resulted in a decrease in functional activity. However, substitution in position 6 resulted in selective and potent ligands. A methoxy moiety was chosen to mimic the oxygen of the compound-**5** benzofuran ring. A series of 6-methoxy-*N*-alkyl isatin acylhydrazone derivatives, based on our previously reported potent CB2 agonists,[38] was prepared and evaluated (Figure 2). The 6-methoxy-*N*-alkyl isatin core was subsequently optimized to find potent selective CB2 inverse agonists. In this report, we describe the design, synthesis, structure−activity relationships, and in vivo and in vitro evaluations of this novel series of potent and selective CB2 inverse agonists. Furthermore, we present the results of molecular modeling studies that we performed in order to suggest a binding mode for this novel class of inverse agonists and to identify residues involved in ligand recognition.

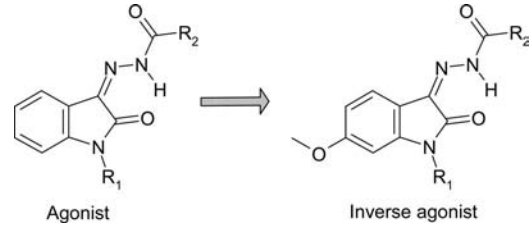

Figure 2. Modification of isatin acylhydrazone that changed CB2 agonists to CB2 inverse agonists.

Methods

Chemistry. The synthesis outlined in Scheme 1 proceeded in two chemical steps from 6-methoxyisatin.[39] *N*-Alkylation of the 6-methoxyisatin with commercially available alkyl halide using cesium carbonate with microwave irradiation in *N*,*N*-dimethylformamide afforded the desired products in good yields. Condensation of the resulting *N*-substituted isatin with hydrazine derivatives afforded the desired hydrazone in good to moderate yields. For hydrazone derivatives **22**, **25**, **26**, and **29**, described below, the ^{1}H nuclear magnetic resonance (NMR) spectra indicated the presence of two rotamers as previously described.[38,40]

Crystallographic Analyses. The structure of compound **15** was examined by X-ray diffraction to confirm the Z configuration. Compound **15** yielded crystals of suitable quality for X-ray diffraction by slow evaporation of an ethyl acetate solution. As expected, the structure obtained (Figure 3) was the one in which the hydrogen borne by nitrogen atom N12 might form a hydrogen bond with oxygen atom O10.

Molecular Modeling Studies. Molecular modeling studies were performed on the 6-methoxyisatin acylhydrazone derivatives to identify a putative binding site of this class of CB2 inverse agonists. There is uncertainty and limited experimental evidence about structure−activity relationships and ligand interactions for CB2-specific inverse agonist compounds.[34,41−45] Depending on ligand chemotypes, the ligand:CB2 interaction

Scheme 1. Synthetic Route[a]

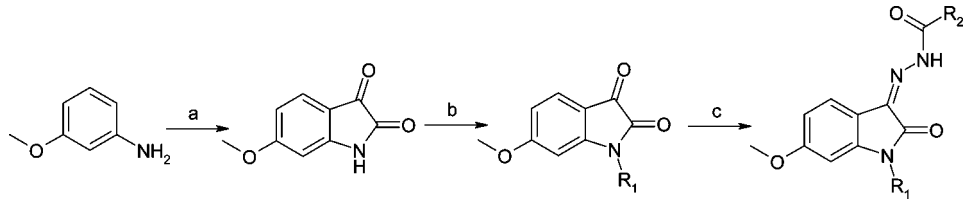

[a] Reagents and conditions: (a) (i) chloral hydrate, hydroxylamine hydrochloride, sodium sulfate, hydrochloric acid, 55 °C, 12 h; (ii) polyphosphoric acid, 55−60 °C, 6 h.[39] (b) $CsCO_3$, *N*,*N*-dimethylformamide, R_1Br, microwave irradiation, 140 °C, 10 min. (c) H_2N-HN-CO-R_2, AcOH, EtOH, tetrahydrofuran, room temperature, 12 h.

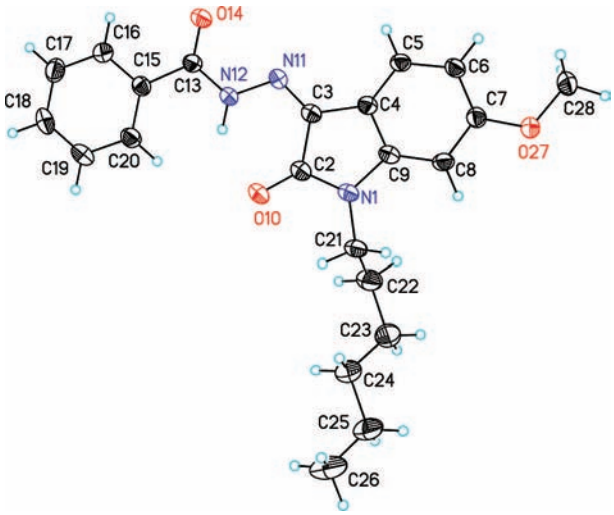

Figure 3. View of compound **15** showing the atom labeling scheme. Displacement ellipsoids are scaled to the 50% probability level.

is considered to be mediated by hydrogen bonds and/or $\pi-\pi$ stacking interactions within transmembrane regions 3−7.[46−48] Thus, the aim of this molecular modeling study was to suggest a binding mode for the isatin acylhydrazone class of CB2-selective inverse agonists and to identify residues involved in ligand recognition.

Pharmacology: Cannabinoid Receptor-Mediated Functional Activity. Functional activity for acyl hydrazone was evaluated using GTPγ[^{35}S] assay in Chinese hamster ovarian cell membrane extracts expressing recombinant human CB1 (*h*CB1) or human CB2 (*h*CB2). The assay relies on the binding of GTPγ[^{35}S], a radiolabeled nonhydrolyzable GTP analogue, to the G protein upon binding of an agonist of the G-protein-coupled receptor. In this system, agonists stimulate GTPγ[^{35}S] binding, whereas antagonists have no effect and inverse agonists decrease GTPγ[^{35}S] basal binding. CB1 and CB2 assay data are presented as the mean of two determinations. Assay reproducibility was monitored by the use of a reference compound, compound **7**. For replicate determinations, the maximum variability tolerated in the test was of ±20% around the average of the replicates. Efficacies (E_{max}) for CB1 and CB2 are expressed as a percentage of the efficacy of compound **7**.

Pharmacology: Binding Assays. Compound **15** was screened in a competitive binding experiment using membranes of CHO-K1 cells selectively expressing *h*CB2 at different concentrations in duplicate.[49] The competitive binding experiment was performed in 96-well plates (Masterblock) containing binding buffer (50 mM Tris, pH 7.4, 2.5 mM EDTA, 0.5% protease-free bovine serum albumin), recombinant membrane extracts (0.25 μg protein/well), and 1 nM [^{3}H]**7** (Perkin-Elmer, NEX-1051, 161 Ci/mmol, diluted in binding buffer). Nonspecific binding was determined in the presence of 10 μM compound **7** (Tocris Bioscience). The sample was incubated in a final volume of 0.1 mL for 60 min at 30 °C and then filtered on a GF/B UniFilter microplate (Perkin-Elmer, catalogue no. 6005177) presoaked in 0.5% polyethyleneimine for 2 h at room temperature. Filters were washed six times with 4 mL of cold binding buffer (50 mM Tris, pH 7.4, 2.5 mM EDTA, 0.5% protease-free bovine serum albumin), and the amount of bound [^{3}H]**7** was determined by liquid scintillation counting. Median inhibition concentration (IC_{50}) values were determined by nonlinear regression using the one-site competition equation. The K_i values were calculated using the Cheng−Prusoff equation ($K_i = IC_{50}/(1 + (L/K_D))$, where L = concentration of radioligand in the assay and K_D = affinity of the radioligand for the receptor.

In Vivo Evaluation: Animals. Adult male Sprague−Dawley rats (Harlan Sprague−Dawley) weighing 120−150 g were used in experimental procedures approved by the Animal Care and Use Committee of The University of Texas M. D. Anderson Cancer Center. Animals were housed three per cage on a 12 h light/12 h dark cycle with water and food pellets available ad libitum.

Lumbar 5/6 Spinal Nerve Ligation Pain Model. All surgical procedures were performed while rats were under deep isoflurane-induced anesthesia in 100% O_2. The spinal nerve ligation was performed as described previously.[50] Briefly, a midline incision was made above the lumbar spine to expose the left L6 transverse process. The process was then removed, the left L5 and L6 spinal nerves were isolated, and both nerves were tightly ligated with 6−0 silk. A prophylactic antibiotic (norfloxacin 5 mg/kg subcutaneously) and a prophylactic analgesic (buprenorphine 0.2−0.5 mg/kg subcutaneously or morphine 2.5 mg/kg subcutaneously) were administered once daily for 3 days. The rats were allowed to recover for 5−6 days before being used for behavioral testings. All the experiments were conducted 10−14 days after spinal nerve ligation.

Assessment of Mechanical Withdrawal Thresholds. For assessment of antiallodynic effect, rats were placed in a compartment with a wire mesh bottom and allowed to acclimate for a minimum of 30 min before testing. Mechanical sensitivity was assessed using a series of Von Frey filaments with logarithmic incremental stiffness (0.41, 0.70, 1.20, 2.00, 3.63, 5.50, 8.50, and 15.1 g) (Stoelting, Wood Dale, IL), as previously described,[51] and 50% probability withdrawal thresholds were calculated with the up−down method.[52] In brief, beginning with the 2.00 g probe, filaments were applied one by one to the plantar surface of a hind paw for 6−8 s. If no withdrawal response was observed, the next stiffer filament was applied; if there was a withdrawal response, the next less stiff filament was applied. Six consecutive responses after the first change in the response were used to calculate the withdrawal threshold (in grams). When response thresholds fell outside the range of detection, 15.00 g was assigned for absence of response to all

tested fibers, and 0.25 g was assigned for withdrawal response to all tested fibers. The percentage maximal possible effect was calculated as ([postdrug threshold − baseline threshold]/[cutoff threshold (15 g) − baseline threshold]) × 100.

Data Analysis. Statistical analyses were carried out using BMDP 2007 (Statistical Solutions, Saugus, MA). Data were analyzed using one-way analysis of variance or *t* test, where appropriate. If findings on analysis of variance were significant, Tukey−Kramer post hoc analysis was used for multiple group comparison. Area under the curve (AUC) was calculated using the trapezoidal rule. The results are presented as mean ± SEM and were considered significant at $P < 0.05$.

Results and Discussion

In our previously published work, we observed that the carbonyl group is essential for CB2 binding of *N*-alkyl isatin acylhydrazone derivatives.[38] Therefore, our first objective in the present study was to find the optimal building blocks for R1 and R2 (Figure 2) needed for CB2 inverse agonist activity. In our previously published agonist series,[38] we noted that the use of benzohydrazide moiety (R2 is a phenyl ring) resulted in compounds with the highest affinities for CB2. Thus, we decided to study first the substituent effect for R1 and in a second step R2.

Recently, Cavasotto et al.[53] developed and validated a method of ligand-steered homology modeling of the binding site in which existing ligands are explicitly used to shape and optimize the binding site through a docking-based stochastic global energy minimization procedure. The ligand and receptor are considered flexible throughout the modeling process, which ensures a better coverage of the energy landscape. This is particularly important in the case of CB2,as there is little structural information available about protein−ligand interactions.[41,46−48,54] To accomplish our aim, we constructed a ligand-steered homology model of CB2 based on the crystal structure of β_2-adrenergic receptor (the approach is summarized in Experimental Section).[55−57] The template structure of β_2 used in our study was crystallized in its inactive state[55−58] hence, the CB2 model obtained may have been in an inactive state suitable for studying the binding of inverse agonist compounds, as suggested by other studies.[48,59]

Generation of a CB2 Model in Agreement with Experimental Evidence. Aromatic and hydrogen bond interactions play an important role in binding of CB2 inverse agonist compounds. Though CB2 models are not as extensively studied as CB1 models, modeling and structure−activity relationship studies have suggested the presence of a hydrophobic pocket within transmembrane regions 3, 5, 6, and 7 surrounded by residues F3.36, W6.48, and W5.43.[41,45,60] Hydrogen bond interactions have also been implicated in binding of antagonists and inverse agonists of CB2.[46,47] However, there is not total agreement on the definition of the binding site and the interactions between different classes of compounds and the receptor.

From the set of compounds displaying inverse agonist activity (Table 1), we selected compound **18** to model the binding site, in accordance with the ligand-steered homology modeling method and similar to what has been done with G protein-coupled receptors and protein kinases.[53,61] Because of the sensitivity of EC_{50} values to substitutions of the R1 group, we hypothesized that the R1 group was facing the interior of the pocket and was not exposed to the free solvent. Thus, in our initial model, the R1 group was oriented toward the hydrophobic pocket. Prior modeling studies for antagonists indicate hydrogen bonding interactions with the serine residues in transmembrane region 4 or with lysine or threonine in transmembrane region 3.[46,47,60] Hence, the R2 group was placed such that it could occupy pockets facing toward transmembrane regions 2 and 3 or transmembrane regions 3, 4, and 5. These two conformations were seeded into the pocket, and an ensemble of 200 structures for each conformation was generated by randomizing the position and orientation of the ligand and then performing a multistep energy minimization in which the van der Waals interaction was gradually switched from soft to full interaction, as performed in other cases.[61−63] The ligand and receptor were held flexible in this stage without any restraints. The structures in the ensemble were then ranked using a crude binding energy estimation (see Experimental Section). Ten structures were subjected to a full flexible-ligand:flexible side chain Monte Carlo-based global energy optimization as has been performed before in G protein-coupled receptors and other proteins.[61−66] From these complexes, two representative structures were chosen on the basis of binding affinity estimation. The binding sites were visually inspected, and the final complex was retained in which the R1 group was oriented toward the lipophilic pocket as described earlier and the carbonyl was positioned close enough to any charged-residue side chain to form a hydrogen bond. As the absence of carbonyl group resulted in lack of affinity for isatin acylhydrazone compounds, we assumed that absence of hydrogen bond interaction with the carbonyl possibly was related to a wrong pose (Figure 4A).

Correlation between Ligand Binding to the CB2 Structural Model and Structure−Activity Relationship Data. Because of the limited experimental evidence available with which to validate our model,[41,46−48,54] we evaluated the accuracy of the model by its ability to explain structure−activity relationship data on our compounds. In our representative model with compound **18** (Figure 4B), the carbonyl group is located at 2 Å from the side chain hydrogen of K3.28, suggesting a possible ligand−receptor interaction via hydrogen bond. Similarly, the location of the methoxy group seems to indicate a hydrogen bond interaction with Y5.39. These observations suggest the possible ligand−receptor interactions and also explain the orientation of the compound. The cyclohexyl moiety is properly located in the hydrophobic pocket to form van der Waals interactions with residues W6.48, F3.36, and W5.43. Specifically, it is important to note the change in affinities with different groups at the R1 position facing toward the aromatic domain. The optimal chain is a *n*-pentyl group because compound **16** was 15 times more potent than compound **15** or compound **17** in terms of efficacy. For compound **16**, the R2 group is oriented toward the lipophilic pocket formed by residues F2.57, F2.61, F2.64, and F7.35, and its overall position suggests favorable aromatic stacking interaction with F2.61 and F2.64. It should be mentioned that as in the agonist series, use of the methylcyclohexyl moiety resulted in loss of selectivity for CB2 compared to CB1. On the other hand, replacing the methylcyclohexyl moiety with a benzyl moiety resulted in restoration of the CB2 selectivity but a decrease in terms of potency for CB2 functional activity. Introducing an oxygen atom in the alkyl chain was poorly tolerated in compound **21** compared to compound **17**. Increasing the length between the cyclohexyl ring and the nitrogen atom, such as in compound **20**, resulted in a dramatic decrease in activity but also restored CB2 selectivity compared to the methylcyclohexyl analogue, compound **18**. This loss of activity might be explained by steric clashes with residues W6.48 and F3.36, which might result in the loss of hydrogen bond interaction with K3.28 or Y5.39.

Table 1. Determination of Potency (EC_{50}) and Maximal Stimulation (E_{max}) on *h*CB1 and *h*CB2 Receptors of Compounds **15**−**29**[a]

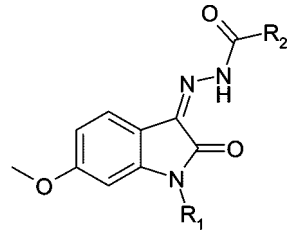

Cpd	R1	R2	GTPγ[^{35}S] (*h*CB1)		GTPγ[^{35}S] (*h*CB2)	
			EC_{50} (nM±SEM)	E_{max} (%)	EC_{50} (nM±SEM)	E_{max} (%)
7			10.3±1	100	8.66±1	100
15	$CH_3(CH_2)_5$	Phenyl	>10 μM	ND	88.2 ± 1.5	-92
16	$CH_3(CH_2)_4$	Phenyl	263 ± 1.8	41.04	5.8 ± 8.8	-108
17	$CH_3(CH_2)_3$	Phenyl	>10 μM	ND	85 ± 1.6	-95
18	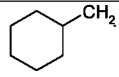	Phenyl	61.2 ± 1.5	40.8	18 ± 1.2	-82
19	Benzyl	Phenyl	>10 μM	ND	102 ± 1.5	-96
20	2-cyclohexylethyl	Phenyl	>10 μM	ND	540 ± 1.3	-104
21	$CH_3O(CH_2)_2$	Phenyl	>10 μM	ND	492±1.2	-60
22	$CH_3(CH_2)_4$	Cyclohexyl	>10 μM	ND	28.7±1.2	-105
23	$CH_3(CH_2)_4$		>10 μM	ND	14.7±1.7	-99
24	$CH_3(CH_2)_4$	-O-tBu	>10 μM	ND	15.9±1.3	-97
25	$CH_3(CH_2)_4$		>10 μM	ND	11.7±1.4	-78
26	$CH_3(CH_2)_4$	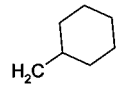	>10 μM	ND	43±1.4	-88
27	$CH_3(CH_2)_4$	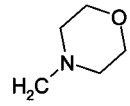	>10 μM	ND	13.3±1.5	-80
28	$CH_3(CH_2)_4$	*tert*-Butyl	>10 μM	ND	10±1.1	-78
29	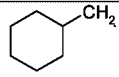	Cyclohexyl	>10 μM	ND	71.6±1.4	-69

[a] CB1 and CB2 assay data are presented as the mean of two determinations. Assay reproducibility was monitored by the use of a reference compound **7**. For replicate determinations, the maximum variability tolerated in the test was of (20% around the average of the replicates). Efficacies (E_{max}) for CB1 or CB2 are expressed as a percentage relative to the efficacy of compound **7**. ND = not determined (plateau was not reached at 10 μM dose).

As the lipophilic pocket formed by residues F2.57, F2.61, F2.64, and F7.35 seemed to be large, we decided to explore the substituent effect for R2, keeping a *n*-pentyl group for R1 as it was the optimal chain length. Replacing the phenyl ring (compound **16**) with a cyclohexyl (compound **22**) or a methylcyclohexyl (compound **26**) resulted in a slight decrease in CB2 functional activity, which might be attributed to a loss of the favorable aromatic stacking interaction with F2.61 and F2.64 and compound **16**. Branched alkyl moieties were slightly better tolerated than the cylohexyl ring, as compounds **23**, **24**, **25**, and **28** had twice the CB2 activity of compound **22**. Introduction of an oxygen atom did not affect the activity (**23**, **24**). Surprisingly,

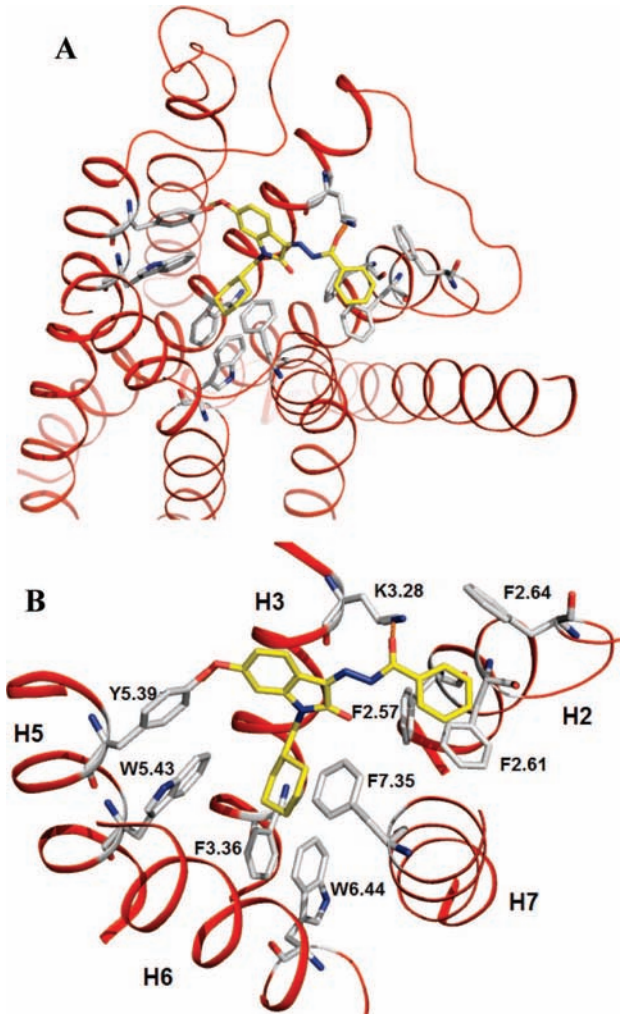

Figure 4. (A) CB2 complexed with compound **18** (yellow carbon atoms). (B) Possible hydrogen bond with K3.28 is represented as orange dashes. The $\pi-\pi$ stacking can be seen with F2.61 and F2.64. Helices are colored in red. Helices 1 and 4 are cut away for clarity. The figure was prepared using PyMol (www.pymol.org).

replacing the methylcyclohexyl moiety of compound **26** with a methylmorpholine (compound **27**) resulted in a 4-fold increase in CB2 functional activity. It is well established that the morpholine ring usually adopts a chair conformation and the four carbon atoms deviate only slightly from coplanarity.[67] The nitrogen of the compound-**27** morpholine ring might form an intramolecular hydrogen bond with the hydrogen atom borne by the hydrazoic moiety.[68] For compound **27**, an additional CH2 group provides flexibility to the morpholine ring, possibly exposing it to the solvent, and hence is well tolerated. The resulting restricted conformation adopted by compound **27** might be greatly different from the conformation adopted by the methylcyclohexyl moiety (**26**) and explain the increase in CB2 activity. Replacing the phenyl ring of compound **18** with a cyclohexyl ring (compound **29**) resulted in a decrease in CB2 activity, probably because of loss of aromatic stacking interaction, as previously mentioned for compound **22**, as well as loss of CB1 functional activity. Aromatic stacking interaction of compound **18** in *h*CB1 seems to be necessary for CB1 functional activity. Compared to compound **22**, compound **29** exhibited a lower CB2 activity, probably because of the rigidity induced by the introduction of two cyclohexyl rings compared to one cyclohexyl and a *n*-pentyl moiety.

The loss of potency for compounds **15** and **17** can be explained as follows. We suggest three possible ligand−receptor interactions: the H-bond with K3.28, the hydrophobic pocket surrounded by W6.48, F3.36, and W5.43, and the $\pi-\pi$ interactions with F2.61 and F2.64. With a shorter carbon chain, like that in compound **17**, the compound may not satisfy all three ligand−receptor interactions, resulting in loss of interactions, whereas with a longer carbon chain, like that in compound **15**, the affinity loss might be explained by steric clashes in the hydrophobic pocket after ligand binding. Compound **16** optimally satisfies all three interactions and thus shows higher affinity. In compound **21**, an unfavorable interaction occurs as a polar atom (oxygen) is introduced in the hydrophobic pocket, resulting in loss of affinity.

A competitive binding assay was also performed in membranes of CHO-K1 cells selectively expressing the *h*CB2 for compound **15**. As expected, compound **15** displaced [^{3}H]**7** from *h*CB2 receptors with a K_i value of 89.9 ± 5.3 nM. In rats, spinal nerve ligation produced tactile allodynia 1 week after surgery, as demonstrated by a reduction in paw withdrawal threshold to mechanical stimulation to 2.3 ± 0.2 g using Von Frey filaments. Intraperitoneal administration of 10 mg/kg or 15 mg/kg of compound **15** did not attenuate tactile allodynia, and the response seen with compound **15** was not different from that seen with its vehicle (*N*-methylpyrrolidone [30%], propylene glycol [30%], ethyl alcohol [10%], Cremophor (10%), and water) (Figure 5A). Nevertheless, intraperitoneal administration of 15 mg/kg of compound **1**, a selective CB2 agonist,[10] resulted in significant antiallodynic effects (Figure 5B) compared with its vehicle (hydroxypropyl-β-cyclodextrin). Intraperitoneal administration of 10 mg/kg of compound **15** 15 min before intraperitoneal administration of compound **1** antagonized the effects of compound **1** (Figure 5B), indicating that compound **15** acts as a CB2 antagonist.

Conclusions

In summary, we have discovered a novel series of CB2 inverse agonists that are potent and selective. A major focus of the optimization effort was to increase the functional activity of this novel series and to avoid potential CB1 central nervous system adverse effects. Compound **15** inhibited the effect of a selective CB2 agonist (compound **1**)[10] in an animal model of neuropathic pain. More potent CB2-selective compounds, such as compound **16**, and compounds with better druglike profiles, such as compound **27**, were also discovered and will be evaluated for their in vivo activities in an in vivo model of inflammation. It should be mentioned that compound **18**, a CB1 agonist and CB2 inverse agonist, exhibited an interesting profile, which we are currently evaluating.

The molecular modeling study presented in this work provides a first study of CB2 based on the structure of β_2-adrenergic receptor. A ligand-based homology model of the CB2 binding site was developed, and on the basis of our results we propose a general binding mode for this class of inverse agonists with CB2. The lipophilic pocket with W6.48, F3.36, V6.51, W5.43, and W5.46 could be involved in van der Waals interactions with the R1 group of the ligands. The R2 group interacts with the hydrophobic pocket surrounded by residues F2.57, F2.61, and F2.64 by $\pi-\pi$ stacking or van der Waals interactions. The model also suggests that residue K3.28 could be involved in hydrogen bonding with the carbonyl group of the ligands or

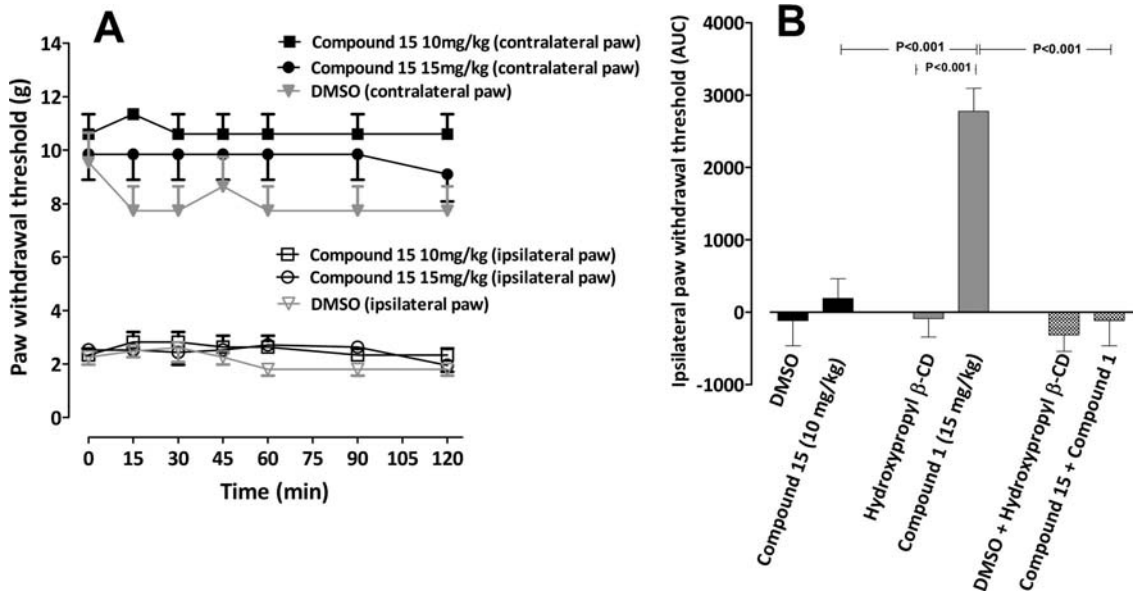

Figure 5. Effects of compound **15** administered by intraperitoneal (ip) injection on tactile allodynia in a spinal nerve ligation neuropathic pain model in rats ($n = 5$ per group). Compound **15** did not have any effect on the withdrawal threshold of the nerve-injured paw (ipsilateral paw) or the normal paw (contralateral paw). (A) The time course of effects of 10 and 15 mg/kg of compound **15**. (B) Area under the curve of the %MPE effects of 10 mg/kg of compound **15** and 15 mg/kg of compound **1**, a selective CB2 agonist. All drugs were administered by ip injection. Administration of 10 mg/kg of compound **15** 15 min before administration of compound **1** antagonized the effects of compound **1** (Figure 5B), indicating that compound **15** acts as a CB2 antagonist.

that Y5.39 could be involved in hydrogen bonding with the methoxy group.

Experimental Section

All chemicals were purchased from Sigma-Aldrich or Acros. Microwave reactions were conducted using an Initiator EXP Microwave System (Biotage, Charlottesville, VA). Thin-layer chromatography analyses were performed on Sigma-Aldrich 60 F254 thin-layer chromatography plates. Column chromatography was performed with silica gel 230−400 mesh. ^{1}H NMR spectra were recorded on a Bruker 300-MHz DPX NMR spectrometer. ^{13}C NMR spectra were recorded on a Bruker 500-MHz DRX NMR spectrometer. Chemical shifts in ppm are reported relative to either residual dimethyl sulfoxide (3.35 ppm) or $CHCl_3$ (7.24 ppm) as internal standards. Signals were abbreviated as follows: s = singlet, br s = broad singlet, d = doublet, t = triplet, q = quadruplet, m = multiplet. Coupling constants (J) are expressed in hertz.

X-ray Diffraction of Compound 15. X-ray experimental data for $C_{21}H_{23}N_3O_2$: Crystals grew as large, yellow plates by slow evaporation of an ethyl acetate solution. The data crystal was cut from a larger crystal and had approximate dimensions of 0.24 mm × 0.20 mm × 0.20 mm. The data were collected at room temperature on a Nonius Kappa charge-coupled device diffractometer using a graphite monochromator with Mo Kα radiation (λ = 0.71073Å). A total of 279 frames of data were collected using ω scans with a scan range of 2° and a counting time of 144 s per frame. The data were collected at 153 K using an Oxford Cryostream low-temperature device. Details of crystal data, data collection, and structure refinement are listed in Table 1. Data reduction was performed using DENZO-SMN.[69] The structure was solved by direct methods using SIR97[70] and refined by full-matrix least-squares on F^2 with anisotropic displacement parameters for the non-H atoms using SHELXL-97.[71] The hydrogen atoms on carbon were calculated in ideal positions with isotropic displacement parameters set to 1.2 × Ueq of the attached atom (1.5 × Ueq for methyl hydrogen atoms). The hydrogen atoms bound to nitrogen were observed in a ΔF map and refined with isotropic displacement parameters. The function $\sum w(|F_o|^2 - |F_c|^2)^2$ was minimized, where $w = 1/[(\sigma(F_o))^2 + (0.0567P)^2 + (0.2659P)]$ and $P = (|F_o|^2 + 2|F_c|^2)/3$. $R_w(F^2)$ refined to 0.119, with $R(F)$ equal to 0.0485 and a goodness of fit, S, = 1.06. Definitions used for calculating $R(F)$, $R_w(F^2)$, and goodness of fit, S, were as follows:

$R(F) = \sum(|F_o| - |F_c|)/\sum|F_o|\}$ for reflections with $F_o > 4(\sigma(F_o))$.

$R_w(F^2) = \{\sum w(|F_o|^2 - |F_c|^2)^2/\sum w(|F_o|)^4\}^{1/2}$, where w is the weight given each reflection.

$S = [\sum w(|F_o|^2 - |F_c|^2)^2/(n - p)]^{1/2}$, where n is the number of reflections and p is the number of refined parameters.

The data were corrected for secondary extinction effects. The correction takes the form: $F_{corr} = kF_c/[1 + (4.2(4) \times 10^{-5})F_c^2 \lambda^3/(\sin 2\theta)]^{0.25,}$ where k is the overall scale factor. Neutral atom scattering factors and values used to calculate the linear absorption coefficient were from the International Tables for X-ray Crystallography (1992).[72] All figures were generated using SHELXTL/PC.[71]

X-ray data for compound **15**. Empirical formula: $C_{22}H_{25}N_3O_3$. Formula weight: 379.45. Temperature: 153(2) K. Wavelength: 0.71070 Å. Crystal system: Triclinic. Space group: $P\bar{1}$. Unit cell dimensions: a = 8.3877(2) Å, α = 100.3570(10)°, b = 8.4043(2) Å, β = 103.5370(10)°, c = 15.1821(4) Å, γ = 101.3700(10)°. Volume: 991.00(4) Å^3. Z = 2. Density (calculated): 1.272 mg/m^3. Absorption coefficient: 0.086 mm^{-1}. F(000) 404. Crystal size: 0.24 mm × 0.20 mm × 0.20 mm. θ range for data collection: 2.58 to 27.47°. Index ranges: $-10 \le h \le 9$, $-10 \le k \le 10$, $-15 \le l \le 19$. Reflections collected: 7232. Independent reflections: 4516 [R(int) = 0.0167]. Completeness to θ = 27.47°, 99.6%. Absorption correction: None. Refinement method: Full-matrix least-squares on F^2. Data/restraints/parameters: 4516/0/259. Goodness-of-fit on F^2: 1.055. Final R indices [$I > 2\sigma(I)$]: R1 = 0.0485, wR2 = 0.1088. R indices (all data): R1 = 0.0688, wR2 = 0.1192. Largest diff peak and hole: 0.390 and −0.227 e·Å^{-3}.

Sequence Alignment and Homology Model of CB2. The CB2 and β_2 sequences were aligned based on existing information on conserved residues within class-A G protein-coupled receptors.[73] CB2 lacks the conserved proline in helix 5, so the next highly conserved residue, tyrosine, was used for the alignment as described by Xie and colleagues.[54] The nomenclature of Ballesteros and colleagues is used, whereby the most conserved residue in helix X is labeled as X.50.[74] The homology model of CB2 was generated using the recently crystallized structure of β_2-adrenergic receptor (PDB code 2RH1) as a template.[55−57] The N- and C-terminus residues (amino acids 1−26 and 316−360) of CB2 and the T4L

residues connecting helixes V and VI of β_2-adrenergic receptor were omitted. The resulting alignment was used as an input to MODELER 9v4[75] to develop a CB2 model. Mutagenesis and other CB2 modeling studies suggest the possibility of disulfide bond between residues Cys 174 and Cys 179 in the E2-loop, which is included in our homology model.[46,47,76] This was followed by a restraint-minimization to relieve the structural strain stemming from the replacement of nonconserved residues in the homology modeling process while keeping the pocket intact. A ligand-steered homology model for CB2 was developed in a way similar to that used to develop a ligand-steerred homology model for the melanin-concentrating hormone receptor, in which existing ligands were explicitly used to shape and optimize the binding site through a docking-based stochastic global energy minimization procedure.[53] Side chains within 6 Å of the ligand were considered free while the backbone was kept fixed and the ligand−receptor binding energy was estimated as the ligand−receptor interaction energy, where the van der Waals, electrostatic, hydrogen bonding, and torsional energy terms were considered.

General Procedure for the Synthesis of the *N*-Alkyl Isatin (General Procedure A). A mixture of cesium carbonate (1.46 g, 4.48 mmol), 6-methoxyisatin[39] (397 mg, 2.24 mmol), and 1-(bromomethyl)cyclohexane (476 mg, 2.69 mmol) in dimethylformamide (20 mL) in sealed vessels was irradiated at 140 °C for 10 min. After extraction with ethyl acetate, the organic layer was washed with hydrochloric acid (0.4N) and water. The organic fraction was dried over $MgSO_4$ and concentrated under vacuum. Compounds **8**−**14** were synthesized using the same quantity as described in this general procedure.

1-Hexyl-6-methoxy-isatin (8). The title compound was prepared as an orange oil, using 6-methoxy-isatin and 1-bromohexane according to general procedure A. Column chromatography (silica gel, heptane/EtOAc: 6/4) afforded the title compound as an orange solid. Yield: 63%. ^{1}H NMR ($CDCl_3$): δ 0.88 (t, J = 6.9 Hz, 3H), 1.33−1.41 (m, 6H), 1.65−1.72 (m, 2H), 3.67 (t, J = 7.5 Hz, 2H), 3.93 (s, 3H), 6.36 (d, J = 1.8 Hz, 1H), 6.54 (dd, J = 1.8 Hz, J = 8.4 Hz, 1H), 7.58 (d, J = 8.4 Hz, 1H).

1-Cyclohexylmethyl-6-methoxy-isatin (9). The title compound was prepared as an orange solid, using 6-methoxy-isatin and 1-bromomethylcyclohexane according to general procedure A. The resulting solid was washed with a mixture of heptane and AcOEt. Yield: 64%; mp: 162−163 °C. ^{1}H NMR ($CDCl_3$): δ 1.01−1.27 (m, 5H), 1.68−1.79 (m, 6H), 3.51 (d, J = 7.5 Hz, 2H), 3.94 (s, 3H), 6.37 (d, J = 2 Hz, 1H), 6.55 (dd, J = 2 Hz, J = 8 Hz, 1H), 7.59 (d, J = 8 Hz, 1H). ^{13}C NMR ($CDCl_3$): δ 25.65 (CH_2), 26.12 (CH_2), 30.90 (CH_2), 36.35 (CH), 46.51 (CH_2), 56.14 (CH_3), 97.99 (CH), 107.24 (CH), 111.34 (C), 128.00 (CH), 154.01 (C), 159.88 (C), 168.19 (C═O), 180.99 (C═O).

1-Benzyl-6-methoxy-isatin (10). The title compound was prepared as an orange solid, using 6-methoxy-isatin and benzyl bromide according to general procedure A. The resulting solid was washed with a mixture of heptane and AcOEt. Yield: 67%; mp: 115.8−116.9 °C. ^{1}H NMR ($CDCl_3$): δ 3.82 (s, 3H), 4.89 (s, 2H), 6.25 (d, J = 2 Hz, 1H), 6.52 (dd, J = 2 Hz, J = 8.5 Hz, 1H), 7.29−7.36 (m, 5H), 7.58 (d, J = 8.5 Hz, 1H). ^{13}C NMR ($CDCl_3$): δ 43.99 (CH_2), 56.04 (CH_3), 98.31 (CH), 107.93 (CH), 111.41 (C), 127.41 (CH), 128.04 (CH), 128.14 (CH), 129.06 (CH), 134.73 (C), 153.22 (C), 159.71 (C), 168.16 (C═O), 180.59 (C═O).

1-Pentyl-6-methoxy-isatin (11). The title compound was prepared as a red solid, using 6-methoxy-isatin and 1-bromopentane according to general procedure A. Column chromatography (silica gel, heptane/EtOAc: 7/3) afforded the title compound as an orange solid. Yield: 57%; mp: 77.6−78.4 °C. ^{1}H NMR ($CDCl_3$): δ 0.91 (t, J = 6.5 Hz, 3H), 1.34−1.39 (m, 4H), 1.67−1.71 (m, 2H), 3.67 (t, J = 7.0 Hz, 2H), 3.93 (s, 3H), 6.37 (d, J = 2 Hz, 1H), 6.55 (dd, J = 2 Hz, J = 8 Hz, 1H), 7.58 (d, J = 8 Hz, 1H). ^{13}C NMR ($CDCl_3$): δ 13.91 (CH_3), 22.29 (CH_2), 27.12 (CH_2), 28.96 (CH_2), 40.17 (CH_2), 56.13 (CH_3), 97.58 (CH), 107.41 (CH), 111.36 (C), 128.04 (CH), 153.52 (C), 159.57 (C), 168.26 (C═O), 181.04 (C═O).

1-Butyl-6-methoxy-isatin (12). The title compound was prepared as a red solid, using 6-methoxy-isatin and 1-bromobutane according to general procedure A. Column chromatography (silica gel, heptane/EtOAc: 6/4) afforded the title compound as an orange solid. Yield: 60%; mp: 70.1 °C. ^{1}H NMR ($CDCl_3$): δ 0.97 (t, J = 7.5 Hz, 3H), 1.38−1.43 (m, 2H), 1.64−1.68 (m, 2H), 3.68 (t, J = 7.0 Hz, 2H), 3.93 (s, 3H), 6.37 (d, J = 2 Hz, 1H), 6.55 (dd, J = 2 Hz, J = 8.5 Hz, 1H), 7.57 (d, J = 8.5 Hz, 1H). ^{13}C NMR ($CDCl_3$): δ 13.69 (CH_3), 20.12 (CH_2), 29.48 (CH_2), 39.94 (CH_2), 56.13 (CH_3), 97.59 (CH), 107.41 (CH), 111.36 (C), 128.04 (CH), 153.52 (C), 159.58 (C), 168.26 (C═O). 181.03 (C═O).

1-(2-Cyclohexylethyl)-6-methoxy-isatin (13). The title compound was prepared as a red solid, using 6-methoxy-isatin and 1-bromo-2-cyclohexylethane according to general procedure A. Column chromatography (silica gel, heptane/EtOAc: 7/3) afforded the title compound as an red solid. Yield: 65%; mp: 94.8 °C. ^{1}H NMR ($CDCl_3$): δ 0.91−1.01 (m, 2H), 1.15−1.31 (m, 4H), 1.55 (q, J = 8.5 Hz, 2H), 1.64−1.73 (m, 3H), 1.79 (d, J = 13 Hz, 2H), 3.69 (t, J = 7.5 Hz, 2H), 3.93 (s, 3H), 6.35 (d, J = 2 Hz, 1H), 6.54 (dd, J = 2 Hz, J = 8.5 Hz, 1H), 7.58 (d, J = 8.5 Hz, 1H). ^{13}C NMR ($CDCl_3$): δ 26.10 (CH_2), 26.40 (CH_2), 33.09 (CH_2), 34.63 (CH_2), 35.38 (CH), 38.12 (CH_2), 56.10 (CH_3), 97.55 (CH), 107.32 (CH), 111.44 (C), 128.06 (CH), 153.44 (C), 159.46 (C), 168.22 (C═O). 181.09 (C═O).

6-Methoxy-1-(2-methoxyethyl)-isatin (14). The title compound was prepared as a red solid, using 6-methoxy-isatin and 1-bromo-2-cyclohexylethane according to general procedure A. Column chromatography (silica gel, heptane/EtOAc: 6/4) afforded the title compound as an orange solid. Yield: 63%; mp: 110.4−11.4 °C. ^{1}H NMR ($CDCl_3$): δ 3.35 (s, 3H), 3.63 (t, J = 5.4 Hz, 2H), 3.87 (t, J = 5.4 Hz, 2H), 3.92 (s, 3H), 6.52−6.56 (m, 2H), 7.56 (dd, J = 1.5, J = 7.5 Hz, 1H).). ^{13}C NMR ($CDCl_3$): δ 40.48 (CH_2), 56.12 (CH_3), 59.04 (CH_3), 70.26 (CH_2), 98.13 (CH), 108.25 (CH), 111.26 (C), 127.72 (CH), 154.14 (C), 159.90 (C), 168.23 (C═O). 180.71 (C═O).

General Procedure for the Synthesis of Hydrazone Derivatives from the Corresponding Isatins (General Procedure B). A solution of isatin derivative (0.5 mmol) and benzhydrazide (68 mg, 0.5 mmol) in a solution of acetic acid 10%, ethanol 45%, and tetrahydrofuran 45% (6.5 mL) was stirred at room temperature for 24 h. The mixture was then concentrated under vacuum to afford the desired product. Compounds **15**−**29** were synthesized using the same quantity as described in this general procedure.

***N′*-[(3*Z*)-1-Hexyl-6-methoxy-2-*oxo*-1,2-dihydro-3*H*-indol-3-ylidene]benzohydrazide (15).** The title compound was prepared as a yellow solid, using 1-hexyl-6-methoxy-isatin and benzhydrazide according to general procedure B. Column chromatography (silica gel, heptane/EtOAc: 5/5) afforded the title compound as a yellow solid. Yield: 74%; mp: 111.4 °C. ^{1}H NMR ($CDCl_3$): δ 0.88 (t, J = 7 Hz, 3H), 1.28 to 1.39 (m, 6H), 1.68−1.74 (m, 2H), 3.73 (t, J = 7.5 Hz, 2H), 3.87 (s, 3H), 6.44 (d, J = 2 Hz, 1H), 6.64 (dd, J = 2 Hz, J = 8 Hz, 1H), 7.51 (t, J = 7.5 Hz, 2H), 7.59 (t, J = 7.5 Hz, 1H), 7.80 (d, J = 8 Hz, 1H), 8.00 (d, J = 7.5 Hz, 1H), 13.98 (br s, 1H).). ^{13}C NMR ($CDCl_3$): δ 13.99 (CH_3), 22.50 (CH_2), 26.63 (CH_2), 27.58 (CH_2), 31.40 (CH_2), 39.97 (CH_2), 55.75 (CH_3), 97.43 (CH), 107.28 (CH), 112.51 (C), 123.67 (CH), 127.74 (CH), 128.91 (CH), 132.38 (C), 132.60 (CH), 137.29 (C), 144.67 (C), 162.56 (C), 163.05 (C), 163.92 (C). Anal. ($C_{22}H_{25}N_3O_3$): C, H, N.

***N′*-[(3*Z*)-6-Methoxy-1-pentyl-2-*oxo*-1,2-dihydro-3*H*-indol-3-ylidene]benzohydrazide (16).** The title compound was prepared as a yellow solid, using 1-pentyl-6-methoxy-isatin and benzhydrazide according to general procedure B. The resulting solid was washed with ethanol. Yellow solid. Yield: 78%; mp:144.8 °C. ^{1}H NMR ($CDCl_3$): δ 0.91 (t, J = 7 Hz, 3H), 1.35 to 1.39 (m, 4H), 1.69−1.75 (m, 2H), 3.73 (t, J = 7.5 Hz, 2H), 3.87 (s, 3H), 6.44 (d, J = 2 Hz, 1H), 6.64 (dd, J = 2 Hz, J = 8.5 Hz 1H), 7.51 (t, J = 7.5 Hz, 2H), 7.59 (t, J = 7.5 Hz, 1H), 7.80 (d, J = 8 Hz 1H), 8.00 (d, J = 7.5 Hz 1H), 13.98 (br s, 1H). ^{13}C NMR ($CDCl_3$): δ 13.92 (CH_3), 22.32 (CH_2), 27.31 (CH_2), 29.05 (CH_2), 39.94 (CH_2), 55.76 (CH_3), 97.43 (CH), 107.28 (CH), 112.51 (C), 123.67 (CH), 127.74

(CH), 132.38 (C), 132.60 (CH), 137.29 (C), 144.67 (C), 162.57 (C), 163.05 (C), 163.92 (C). Anal. ($C_{21}H_{23}N_3O_3$): C, H, N.

***N′*-[(3*Z*)-1-Butyl-6-methoxy-2-*oxo*-1,2-dihydro-3*H*-indol-3-ylidene]benzohydrazide (17).** The title compound was prepared as a yellow solid, using 1-butyl-6-methoxy-isatin and benzhydrazide according to general procedure B. The resulting solid was washed with ethanol. Yellow solid. Yield: 70%; mp: 183.2 °C. ^{1}H NMR ($CDCl_3$): δ 0.98 (t, J = 5 Hz, 1H), 1.38 to 1.45 (m, 4H), 1.67−1.73 (m, 2H), 3.73 (t, J = 7 Hz, 2H), 3.87 (s, 3H), 6.44 (d, J = 2 Hz, 1H), 6.64 (dd, J = 2, Hz, J = 8.5 Hz, 1H), 7.51 (t, J = 7.5 Hz, 2H), 7.59 (t, J = 7.5 Hz, 1H), 7.80 (d, J = 8 Hz, 1H), 8.00 (d, J = 7.5 Hz, 2H), 13.97 (br s, 1H). ^{13}C NMR ($CDCl_3$): δ 13.71 (CH_3), 20.23 (CH_2), 29.67 (CH_2), 39.70 (CH_2), 55.76 (CH_3), 97.44 (CH), 107.28 (CH), 112.50 (C), 123.66 (CH), 127.73 (CH), 128.90 (CH), 132.38 (C), 132.60 (CH), 137.27 (C), 144.67 (C), 162.59 (C), 163.05 (C). 163.93 (C). Anal. ($C_{20}H_{21}N_3O_3$): C, H, N.

***N′*-[(3*Z*)-1-(Cyclohexylmethyl)-6-methoxy-2-*oxo*-1,2-dihydro-3*H*-indol-3-ylidene]benzohydrazide (18).** The title compound was prepared as a yellow solid, using 1-cyclohexylmethyl-6-methoxy-isatin and benzhydrazide according to general procedure B. The resulting solid was washed with ethyl acetate. Yellow solid. Yield: 69%; mp: 220 °C. ^{1}H NMR ($CDCl_3$-d_6): δ 1.01−1.09 (m, 2H), 1.16 to 1.26 (m, 3H), 1.68−1.86 (m, 6H), 3.56 (d, 2H), 6.44 (d, 1H), 6.64 (dd, 1H), 7.51 (t, 2H), 7.58 (t, 1H), 7.80 (d, 1H), 8.01 (d, 2H), 13.98 (br s, 1H). Anal. ($C_{23}H_{25}N_3O_3$): C, H, N.

***N′*-[(3*Z*)-1-Benzyl-6-methoxy-2-*oxo*-1,2-dihydro-3*H*-indol-3-ylidene]benzohydrazide (19).** The title compound was prepared as a yellow solid, using 1-benzyl-6-methoxy-isatin and benzhydrazide according to general procedure B. The resulting solid was washed with ethyl alcohol. Yellow solid. Yield: 62%; mp: 186.2−186.7 °C. ^{1}H NMR ($CDCl_3$): δ 3.77 (s, 3H), 4.94 (s, 2H), 6.35 (d, J = 2 Hz, 1H), 6.62 (dd, J = 2 Hz, J = 8 Hz, 1H), 7.29−7.36 (m, 4H), 7.51 (t, J = 7.5 Hz, 2H), 7.59 (t, J = 7.5 Hz, 1H), 7.80 (d, J = 8 Hz, 1H), 8.01 (d, J = 7.5 Hz, 2H), 13.95 (br s, 1H). ^{13}C NMR ($CDCl_3$): δ 43.55 (CH_2), 55.67 (CH_3), 97.99 (CH), 107.71 (CH), 112.46 (C), 123.63 (CH), 127.30 (CH), 127.76 (CH), 128.11 (CH), 128.92 (CH), 129.06 (CH), 132.33 (C), 132.67 (CH), 137.01 (C), 144.43 (C), 162.63 (C), 162.96 (C), 163.94 (C). Anal. ($C_{23}H_{19}N_3O_3$): C, H, N.

***N′*-[(3*Z*)-1-(2-Cyclohexylethyl)-6-methoxy-2-*oxo*-1,2-dihydro-3*H*-indol-3-ylidene]benzohydrazide (20).** The title compound was prepared as a yellow solid, using 1-(2-cyclohexylethyl)-6-methoxy-isatin and benzhydrazide according to general procedure B. The resulting solid was washed with ethanol. Yellow solid. Yield: 69%; mp: 179−180.8 °C. ^{1}H NMR ($CDCl_3$): δ 0.96−1.04 (m, 2H), 1.15−1.38 (m, 4H), 1.59 (q, J = 7.5 Hz 2H), 1.65−1.75 (m, 3H), 1.81 (d, J = 12.5 Hz 2H), 3.74 (t, J = 7.5 Hz, 2H), 3.87 (s, 3H), 6.43 (d, J = 2 Hz, 1H), 6.64 (dd, J = 2 Hz, J = 8 Hz, 1H), 7.51 (t, J = 7.5 Hz, 2H), 7.59 (t, J = 7.5 Hz, 1H), 7.80 (d, J = 8 Hz, 1H), 8.00 (d, J = 7.5 Hz, 1H), 13.96 (br s, 1H). ^{13}C NMR ($CDCl_3$): δ 26.10 (CH_2), 26.40 (CH_2), 33.10 (CH_2), 34.82 (CH_2), 35.51 (CH), 37.89 (CH_2), 55.74 (CH_3), 97.39 (CH), 107.23 (CH), 112.58 (C), 123.67 (CH), 127.75 (CH), 128.91 (CH), 132.40 (C), 132.59 (CH), 137.31 (C), 144.6 (C), 162.45 (C), 163.05 (C), 163.92 (C). Anal. ($C_{24}H_{27}N_3O_3$): C, H, N.

***N′*-[(3*Z*)-6-Methoxy-1-(2-methoxyethyl)-2-*oxo*-1,2-dihydro-3*H*-indol-3-ylidene] benzohydrazide (21).** The title compound was prepared as a yellow solid, using 6-methoxy-1-(2-methoxyethyl)-isatin and benzhydrazide according to general procedure B. The resulting solid was washed with ethanol. Yellow solid. Yield: 66%; mp: 168−169 °C. ^{1}H NMR ($CDCl_3$): δ 3.35 (s, 3H), 3.65 (t, 2H), 3.87 (s, 3H), 3.94 (t, 2H), 6.64 (d, 1H), 7.58 (t, 1H), 7.79 (d, 1H), 13.93 (br s, 1H). ^{13}C NMR ($CDCl_3$): δ 40.03 (CH_2), 56.73 (CH_3), 59.14 (CH_3), 69.76 (CH_2), 97.72 (CH), 107.84 (CH), 112.33 (C), 123.49 (CH), 127.73 (CH), 128.89 (CH), 132.32 (C), 132.63 (CH), 137.17 (C), 144.93 (C), 162.81 (C), 163.04 (C), 163.91 (C). Anal. ($C_{19}H_{19}N_3O_4$): C, H, N.

***N′*-[(3*Z*)-6-Methoxy-1-pentyl-2-*oxo*-1,2-dihydro-3*H*-indol-3-ylidene]cyclohexanecarbohydrazide (22).** The title compound was prepared as a yellow solid, using 1-pentyl-6-methoxy-isatin and cyclohexanecarbohydrazide according according to general procedure B. The resulting solid was washed with ethanol. Yellow solid. Yield: 32%; mp: 99.6 °C. ^{1}H NMR ($CDCl_3$): δ 0.91 (t, J = 6 Hz, 3H), 1.25 to 1.37 (m, 7H), 1.54−1.60 (m, 3H), 1.70−1.72 (m, 2H), 1.82−1.85 (m, 2H), 1.89 (d, J = 12 Hz, 0.6H, minor isomer) and 2.00 (d, J = 12 Hz, 1.4H, major isomer), 2.34 (t, J = 12 Hz, 0.6H, major isomer) and 3.33 (t, J = 12 Hz, 0.4H, minor isomer), 3.70 (t, J = 7.5 Hz, 2H), 3.87 (s, 3H), 6.43 (d, J = 2 Hz, 1H), 6.61 (d, J = 8.5 Hz, 1H), 7.51 (d, J = 8.5 Hz, 0.4H, minor isomer), and 7.73 (d, J = 8.5 Hz, 0.6H, major isomer), 12.28 (br s 0.4H, minor isomer) and 13.078 (br s 0.6H, major isomer). ^{13}C NMR ($CDCl_3$): δ 13.91 (CH_3), 22.31 (CH_2), 25.64 (CH_2), 25.75 (CH_2), 25.95 (CH_2), 27.27 (CH_2), 28.80 (CH_2) and 29.06 (CH_2) for 2 isomers, 29.41 (CH_2), 39.22 (CH_2) and 39.63 (CH_2) for 2 isomers, 39.88 (CH_2), 44.72 (CH), 55.73 (CH_3), 96.96 (CH) and 97.36 (CH) for 2 isomers, 107.16 (CH), 112.61 (C) and 112.98 (C) for 2 isomers, 121.91 (CH) and 123.52 (CH) for 2 isomers, 132.25 (C) and 136.42 (C) for 2 isomers, 144.54 (C), 161.49 (C) and 162.36 (C) for 2 isomers, 162.50 (C) and 162.90 (C) for 2 isomers, 173.30 (C) and 178.86 (C) for 2 isomers. Anal. ($C_{21}H_{29}N_3O_3$): C, H, N.

2-Hydroxy-*N′*-[(3*Z*)-6-methoxy-1-pentyl-2-*oxo*-1,2-dihydro-3*H*-indol-3-ylidene]-2-methylpropanohydrazide (23). The title compound was prepared as a yellow solid, using 1-pentyl-6-methoxy-isatin and 2-hydroxy-2-methylpropanohydrazide according to general procedure B. Column chromatography (silica gel, heptane/EtOAc: 4/6) afforded the title compound as a yellow solid. Yield: 86%; mp: 133.2 °C. NMR ($CDCl_3$): δ 0.91 (t, J = 6.5 Hz, 3H), 1.34 to 1.36 (m, 4H), 1.59 (s, 6H), 1.66−1.75 (m, 2H), 2.63 (s, 1H), 3.68 (t, J = 7 Hz, 2H), 3.87 (s, 3H), 6.41 (d, J = 2 Hz, 1H), 6.61 (dd, J = 2 Hz, J = 8.5 Hz, 1H), 7.73 (d, J = 8.5 Hz 1H), 13.71 (br s, 1H). ^{13}C NMR ($CDCl_3$): δ 13.90 (CH_3), 22.30 (CH_2), 27.25 (CH_2), 28.06 (CH_3), 29.04 (CH_2), 39.89 (CH_2), 55.74 (CH_3), 73.75 (C), 97.33 (CH), 107.14 (CH), 112.47 (C), 123.70 (CH), 137.84 (C), 144.85 (C), 162.01 (C), 163.12 (C), 174.11 (C). Anal. ($C_{18}H_{25}N_3O_4 \cdot 0.015$heptane): C, H, N.

***tert*-Butyl-(2*Z*)-2-(6-methoxy-1-pentyl-2-*oxo*-1,2-dihydro-3*H*-indol-3-ylidene)hydrazinecarboxylate (24).** The title compound was prepared as a yellow solid, using 1-pentyl-6-methoxy-isatin and *tert*-butyl carbazate according to general procedure B. Column chromatography (silica gel, heptane/EtOAc: 5/5) afforded the title compound as a yellow solid. Yield: 54%; mp: 105.3 °C. ^{1}H NMR ($CDCl_3$): δ 0.91 (t, J = 6.5 Hz, 3H), 1.36 to 1.39 (m, 4H), 1.67−1.70 (m, 2H), 3.70 (t, J = 7 Hz, 2H), 3.86 (s, 3H), 6.41 (d, J = 2 Hz, 1H), 6.60 (dd, J = 2 Hz, J = 8 Hz, 1H), 7.66 (d, J = 8 Hz, 1H), 12.201 (br s, 1H). ^{13}C NMR ($CDCl_3$): δ 13.91 (CH_3), 22.30 (CH_2), 27.28 (CH_2), 28.17 (CH_3), 29.03 (CH_2), 39.74 (CH_2), 55.69 (CH_3), 82.15 (C), 97.08 (CH), 106.96 (CH), 112.97 (C), 122.68 (CH), 144.07 (C), 152.49 (C), 162.16 (C), 162.33 (C). Anal. ($C_{19}H_{27}N_3O_4$): C, H, N.

***N′*-[(3*Z*)-6-Methoxy-1-pentyl-2-*oxo*-1,2-dihydro-3*H*-indol-3-ylidene]-3-methylbutanohydrazide (25).** The title compound was prepared as a yellow solid, using 1-pentyl-6-methoxy-isatin and 3-methylbutanohydrazide according to general procedure B. Column chromatography (silica gel, heptane/EtOAc: 6/4) afforded the title compound as a yellow solid. Yield: 64%; mp: 47.8−49.4 °C. ^{1}H NMR ($CDCl_3$): δ 0.92 (t, J = 2 Hz, 3H), 1.05 (d, J = 6.5 Hz, 6H), 1.36 to 1.39 (m, 4H), 1.69−1.75 (m, 2H), 2.30 (m, 2H), 2.72 (d, J = 6.5 Hz, 1H), 3.72 (t, J = 7 Hz, 2H), 3.89 (s, 3H), 6.44 (d, J = 2 Hz, 1H), 6.64 (m, 1H), 7.54 (d, J = 8 Hz, 1/2H) and 7.77 (d, J = 8 Hz, 1/2H) for 2 isomers, 12.41 and 13.03 (br s for isomers, 1H). ^{13}C NMR ($CDCl_3$): δ 13.91 (CH_3), 22.29 (CH_2), 22.51 (CH_3) and 22.71 (CH_3) for 2 isomers, 25.35 (CH) and 26.25 (CH) for 2 isomers, 27.27 (CH_2), 28.98 (CH_2) and 29.04 (CH_2) for 2 isomers, 39.69 (CH_2) and 39.84 (CH_2) for 2 isomers, 40.45 (CH_2) and 44.85 (CH_2) for 2 isomers, 55.72 (CH_3), 96.93 (CH) and 97.36 (CH) for 2 isomers, 107.07 (CH) and 107.15 (CH) for 2 isomers, 112.51 (C) and 112.92 (C) for 2 isomers, 121.94 (CH) and 123.54 (CH) for 2 isomers, 132.36 (C) and 136.24 (C) for 2 isomers, 144.60 (C), 161.49 (C) and 162.33 (C) for 2 isomers, 162.53 (C) and 162.95 (C) for 2 isomers, 169.76 (C) and 175.51 (C) for 2 isomers. Anal. ($C_{19}H_{27}N_3O_3$): C, H, N.

2-Cyclohexyl-*N*′-[(3*Z*)-6-methoxy-1-pentyl-2-*oxo*-1,2-dihydro-3*H*-indol-3-ylidene]acetohydrazide (26). The title compound was prepared as a yellow solid, using 1-pentyl-6-methoxy-isatin and 2-cyclohexylacetohydrazide according to general procedure B. Column chromatography (silica gel, heptane/EtOAc: 5/5) afforded the title compound as a yellow solid. Yield: 84%; mp: 63.5 °C. ^{1}H NMR ($CDCl_3$): δ 0.91 (t, J = 5.5 Hz, 3H), 1.01−1.07 (m, 2H), 1.18 to 1.39 (m, 7H), 1.60−1.72 (m, 5H), 1.81 (d, J = 12 Hz, 2 H), 1.92−1.94 (m, 1H), 2.27 (d, J = 7 Hz, 1H), 2.69 (d, J = 7 Hz, 1H), 3.70 (t, J = 5.5 Hz, 2H), 3.87 (s, 3H), 6.42 (s, 1H), 6.62 (d, J = 8 Hz, 1H), 7.52 (d, J = 8 Hz, 1/2H) and 7.74 (d, J = 8 Hz, 1/2H) for 2 isomers, 12.39 (br s, 1/2H) and 13.99 (br s, 1/2H) for 2 isomers. ^{13}C NMR ($CDCl_3$): δ 13.91 (CH_3), 22.29 (CH_2), 25.97 (CH_2) and 26.15 (CH_2) for 2 isomers, 26.29 (CH_2), 27.27 (CH_2), 28.99 (CH_2) and 29.04 (CH_2) for 2 isomers, 33.13 (CH_2) and 33.32 (CH_2) for 2 isomers, 34.66 (CH) and 35.44 (CH) for 2 isomers, 39.05 (CH_2), 39.69 (CH_2) and 39.84 (CH_2) for 2 isomers, 43.66 (CH_2), 55.72 (CH_3), 96.99 (CH) and 97.34 (CH) for 2 isomers, 107.07 (CH) and 107.14 (CH) for 2 isomers, 112.51 (C) and 112.95 (C) for 2 isomers, 121.95 (CH) and 123.54 (CH) for 2 isomers, 132.36 (C) and 136.20 (C) for 2 isomers, 144.59 (C), 161.48 (C) and 162.32 (C) for 2 isomers, 162.52 (C) and 162.94 (C) for 2 isomers, 169.75 (C) and 175.52 (C) for 2 isomers. Anal. ($C_{22}H_{31}N_3O_3$): C, H, N.

***N*′-[(3*Z*)-6-Methoxy-1-pentyl-2-*oxo*-1,2-dihydro-3*H*-indol-3-ylidene]-2-morpholin-4-ylacetohydrazide (27).** The title compound was prepared as a yellow solid, using 1-pentyl-6-methoxy-isatin and 2-morpholin-4-ylacetohydrazide according to general procedure B. Column chromatography (silica gel, heptane/EtOAc: 3/7) afforded the title compound as a yellow solid. Yield: 85%; mp: 97.1 °C. ^{1}H NMR ($CDCl_3$): δ 0.92 (t, J = 6.5 Hz, 3H), 1.36 to 1.39 (m, 4H), 1.67−1.72 (m, 2H), 2.61 (t, J = 4 Hz, 4H), 3.29 (s, 2H), 3.70 (t, J = 6.5 Hz, 2H), 3.85 (t, J = 4 Hz, 4H), 3.87 (s, 3H), 6.41 (d, J = 1.5, 1H), 6.60 (dd, J = 1.5, Hz, J = 8 Hz, 1H), 7.75 (d, J = 8 Hz, 2H), 13.86 (br s, 1H). ^{13}C NMR ($CDCl_3$): δ 13.93 (CH_3), 22.27 (CH_2), 27.23 (CH_2), 28.93 (CH_2), 29.72 (CH_2), 53.91 (CH_2), 55.73 (CH_3), 61.59 (CH_2), 66.80 (CH_2), 97.24 (CH), 106.96 (CH), 112.53 (C), 123.64 (CH), 137.68 (C), 145.00 (C), 161.96 (C), 163.11 (C), 168.19 (C). Anal. ($C_{20}H_{28}N_4O_4$): C, H, N.

***N*′-[(3*Z*)-6-Methoxy-1-pentyl-2-*oxo*-1,2-dihydro-3*H*-indol-3-ylidene]-2,2-dimethylpropanohydrazide (28).** The title compound was prepared as a yellow solid, using 1-pentyl-6-methoxy-isatin and 2,2-dimethylpropionic acid hydrazide according to general procedure B. Column chromatography (silica gel, heptane/EtOAc: 5/5) afforded the title compound as a yellow solid. Yield: 98%; mp: 56.3 °C. ^{1}H NMR ($CDCl_3$): δ 0.91 (t, J = 6.5 Hz, 3H), 1.36 to 1.39 (m, 13H), 1.69−1.75 (m, 2H), 3.70 (t, J = 7.5 Hz, 2H), 3.87 (s, 3H), 6.42 (d, J = 2 Hz, 1H), 6.62 (dd, J = 2 Hz, J = 8 Hz, 1H), 7.74 (d, J = 8 Hz, 2H), 13.34 (br s, 1H). ^{13}C NMR ($CDCl_3$): δ 13.91 (CH_3), 22.31 (CH_2), 27.29 (CH_2), 27.39 (CH_3), 29.04 (CH_2), 39.00 (C), 39.88 (CH_2), 55.72 (CH_3), 97.33 (CH), 107.15 (CH), 112.62 (C), 123.90 (CH), 136.80 (C), 144.58 (C), 162.35 (C), 162.87 (C), 175.79 (C). Anal. ($C_{19}H_{27}N_3O_3$·0.04heptane): C, H, N.

***N*′-[(3*Z*)-1-(Cyclohexylmethyl)-6-methoxy-2-*oxo*-1,2-dihydro-3*H*-indol-3-ylidene]cyclohexanecarbohydrazide (29).** The title compound was prepared as a yellow solid, using 1-pentyl-6-methoxy-isatin and cyclohexanecarbohydrazide according to general procedure B. The resulting solid was washed with ethanol. Column chromatography (silica gel, heptane/EtOAc: 5/5) afforded the title compound as a yellow solid. Yield: 70%; mp: 147.5 °C. ^{1}H NMR ($CDCl_3$): δ 1.02−1.07 (m, 2H), 1.19−1.33 (m, 6H), 1.54−1.61 (m, 3H), 1.70−1.88 (m, 9H), 1.89 (d, J = 12 Hz, 0.66H, minor isomer) and 2.00 (d, J = 12 Hz, 1.33H, major isomer), 2.33 (t, J = 12 Hz, 0.6H, major isomer) and 3.33 (t, J = 12 Hz, 0.4H, minor isomer), 3.53 (d, J = 7 Hz, 2H), 3.87 (s, 3H), 6.42 (d, J = 1.5 Hz, 1H), 6.62 (d, J = 8.5 Hz, 1H), 7.52 (d, J = 8.5 Hz, 0.4H, minor isomer), and 7.73 (d, J = 8.5 Hz, 0.6H, major isomer), 12.29 (br s 0.4H, minor isomer) and 13.07 (br s 0.6H, major isomer). ^{13}C NMR ($CDCl_3$): δ 25.66 (CH_2), 25.74 (CH_2), 25.95 (CH_2), 26.14 (CH_2), 28.79 (CH_2) and 29.39 (CH_2) for 2 isomers, 30.94 (CH_2) and 31.02 (CH_2) for 2 isomers, 36.50 (CH_2) and 39.21 (CH_2) for 2 isomers, 44.71 (CH), 46.04 (CH_2) and 46.25 for 2 isomers, 55.74 (CH_3), 97.38 (CH) and 97.77 (CH) for 2 isomers, 106.89 (CH) and 106.99 (CH) for 2 isomers, 112.55 (C) and 112.93 (C) for 2 isomers, 121.81 (CH) and 123.42 (CH) for 2 isomers, 132.16 (C) and 136.32 (C) for 2 isomers, 145.02 (C), 161.79 (C) and 162.43 (C) for 2 isomers, 162.66 (C) and 162.82 (C) for 2 isomers, 173.29 (C) and 178.81 (C) for 2 isomers. Anal. ($C_{23}H_{31}N_3O_3$·0.015heptane): C, H, N.

In Vitro Receptor Radioligand Binding Studies. Compound **15** was also screened in a competitive binding experiment by using membranes of CHO-K1 cells selectively expressing *h*CB_2 at different compound-**15** concentrations in duplicate.[49] The competitive binding experiment was performed in 96-well plates (Masterblock) containing binding buffer (50 mM Tris, pH 7.4, 2.5 mM EDTA, 0.5% protease-free bovine serum albumin), recombinant membrane extracts (0.25 μg protein/well), and 1 nM [^{3}H]**7** (Perkin-Elmer, NEX-1051, 161 Ci/mmol, diluted in binding buffer). Nonspecific binding was determined in the presence of 10 μM compound **7** (Tocris Bioscience). The sample was incubated in a final volume of 0.1 mL for 60 min at 30 °C and then filtered on a GF/B UniFilter microplate (Perkin-Elmer, catalogue no. 6005177) presoaked in 0.5% polyethyleneimine for 2 h at room temperature. Filters were washed six times with 4 mL of cold binding buffer (50 mM Tris, pH 7.4, 2.5 mM EDTA, 0.5% protease-free bovine serum albumin), and bound [^{3}H]**7** was determined by liquid scintillation counting. The median inhibition concentration (IC_{50}) was determined by nonlinear regression by using the one-site competition equation. The inhibition constant (K_i) values were calculated by using the Cheng−Prusoff equation [$K_i = IC_{50}/(1 + (L/K_D)$], where L = concentration of radioligand in the assay and K_D = affinity of the radioligand for the receptor.

[^{35}S]GTP-γ-S Functional Assays. Functional activity was evaluated using GTPγ[^{35}S] assay in Chinese hamster ovarian cell membrane extracts expressing recombinant *h*CB1 or *h*CB2. The assay relies on the binding of GTPγ[^{35}S], a radiolabeled nonhydrolyzable GTP analogue, to the G protein upon binding of an agonist of the G-protein-coupled receptor. In this system, agonists stimulate GTPγ[^{35}S] binding, whereas antagonists have no effect and inverse agonists decrease GTPγ[^{35}S] basal binding.

Compounds were solubilized in 100% dimethyl sulfoxide at a concentration of 10 mM within 4 h of the first testing session (master solution). A predilution for the dose−response curve was performed in 100% dimethyl sulfoxide and then diluted 100-fold in assay buffer at a concentration 4-fold higher than the concentration to be tested. Compounds were tested for agonist activity at eight concentrations in duplicate: 10, 3, 1, 0.3, 0.1, 0.03, 0.01, and 0.001 μM, with compound **7** (Tocris, 0949) as the reference agonist. For GTPγ[^{35}S], membranes (Euroscreen SA, Gosselies, Belgium) were mixed with GDP diluted in assay buffer to give 30 μM solution (volume:volume) and incubated for at least 15 min on ice. In parallel, GTP-γ-[^{35}S] (Amersham, SJ1308) was mixed with PVT-WGA beads (Amersham, RPNQ001) diluted in assay buffer at 50 mg/mL (0.5 mg/10 μL) (volume:volume) just before the reaction was started. The following reagents were successively added in the wells of an Optiplate (Perkin-Elmer): 50 μL of ligand, 20 μL of the membranes:GDP mix, 10 μL of assay buffer for agonist testing, and 20 μL of the GTP-γ-[^{35}S]:beads mix. The plates were covered with a topseal, shaken on an orbital shaker for 2 min, and then incubated for 1 h at room temperature. Then the plates were centrifuged for 10 min at 2000 rpm, incubated at room temperature for 1 h, and counted for 1 min/well with a PerkinElmer TopCount reader. Assay reproducibility was monitored by the use of a reference compound **7**. For replicate determinations, the maximum variability tolerated in the test was of ±20% around the average of the replicates. Efficacies (E_{max}) for CB1 and CB2 are expressed as a percentage relative to the efficacy of compound **7**.

Acknowledgment. We thank Dr. Kumar Kaluarachchi for performing the two-dimensional NMR studies. The NMR Facility at M. D. Anderson Cancer Center is supported by

Cancer Center Support Grant CA16672 awarded by the National Cancer Institute.

Supporting Information Available: Crystallographic data for compound **15**, elemental analyses, and ^{1}H NMR spectra for compounds **15**−**29**. This material is available free of charge via the Internet at http://pubs.acs.org.

References

(1) Karsak, M.; Gaffal, E.; Date, R.; Wang-Eckhardt, L.; Rehnelt, J.; Petrosino, S.; Starowicz, K.; Steuder, R.; Schlicker, E.; Cravatt, B.; Mechoulam, R.; Buettner, R.; Werner, S.; Di Marzo, V.; Tuting, T.; Zimmer, A. Attenuation of allergic contact dermatitis through the endocannabinoid system. *Science* **2007**, *316*, 1494–1497.

(2) Petrosino, S.; Palazzo, E.; de Novellis, V.; Bisogno, T.; Rossi, F.; Maione, S.; Di Marzo, V. Changes in spinal and supraspinal endocannabinoid levels in neuropathic rats. *Neuropharmacology* **2007**, *52*, 415–422.

(3) Jhaveri, M. D.; Richardson, D.; Kendall, D. A.; Barrett, D. A.; Chapman, V. Analgesic effects of fatty acid amide hydrolase inhibition in a rat model of neuropathic pain. *J. Neurosci.* **2006**, *26*, 13318–13327.

(4) Matsuda, L. A.; Lolait, S. J.; Brownstein, M. J.; Young, A. C.; Bonner, T. I. Structure of a cannabinoid receptor and functional expression of the cloned cDNA. *Nature* **1990**, *346*, 561–564.

(5) Munro, S.; Thomas, K. L.; Abu-Shaar, M. Molecular characterization of a peripheral receptor for cannabinoids. *Nature* **1993**, *365*, 61–65.

(6) Herkenham, M.; Lynn, A. B.; Little, M. D.; Johnson, M. R.; Melvin, L. S.; de Costa, B. R.; Rice, K. C. Cannabinoid Receptor Localization in Brain. *Proc. Natl Acad. Sci. U.S.A.* **1990**, *87*, 1932–1936.

(7) Ameri, A. The effects of cannabinoids on the brain. *Prog. Neurobiol.* **1999**, *58*, 315–348.

(8) Facci, L.; Dal Toso, R.; Romanello, S.; Buriani, A.; Skaper, S. D.; Leon, A. Mast cells express a peripheral cannabinoid receptor with differential sensitivity to anandamide and palmitoylethanolamide. *Proc. Natl Acad. Sci. U.S.A.* **1995**, *92*, 3376–3380.

(9) Yao, B. B.; Hsieh, G. C.; Frost, J. M.; Fan, Y.; Garrison, T. R.; Daza, A. V.; Grayson, G. K.; Zhu, C. Z.; Pai, M.; Chandran, P.; Salyers, A. K.; Wensink, E. J.; Honore, P.; Sullivan, J. P.; Dart, M. J.; Meyer, M. D. In vitro and in vivo characterization of A-796260: a selective cannabinoid CB2 receptor agonist exhibiting analgesic activity in rodent pain models. *Br. J. Pharmacol.* **2008**, *153*, 390–401.

(10) Naguib, M.; Diaz, F.; Xu, J.; Astruc-Diaz, F.; Craig, S.; Vivas-Mejia, P.; Brown, D. L. MDA7: A novel selective agonist for CB2 receptors that prevents allodynia in rat neuropathic pain models. *Br. J. Pharmacol.* **2008**, *155*, 1104–1116.

(11) Wotherspoon, G.; Fox, A.; McIntyre, P.; Colley, S.; Bevan, S.; Winter, J. Peripheral nerve injury induces cannabinoid receptor 2 protein expression in rat sensory neurons. *Neuroscience* **2005**, *135*, 235–245.

(12) Beltramo, M.; Bernardini, N.; Bertorelli, R.; Campanella, M.; Nicolussi, E.; Fredduzzi, S.; Reggiani, A. CB2 receptor-mediated antihyperalgesia: possible direct involvement of neural mechanisms. *Eur. J. Neurosci.* **2006**, *23*, 1530–1538.

(13) Zhang, J.; Hoffert, C.; Vu, H. K.; Groblewski, T.; Ahmad, S.; O'Donnell, D. Induction of CB2 receptor expression in the rat spinal cord of neuropathic but not inflammatory chronic pain models. *Eur. J. Neurosci.* **2003**, *17*, 2750–2754.

(14) Walczak, J. S.; Pichette, V.; Leblond, F.; Desbiens, K.; Beaulieu, P. Behavioral, pharmacological and molecular characterization of the saphenous nerve partial ligation: a new model of neuropathic pain. *Neuroscience* **2005**, *132*, 1093–1102.

(15) Walczak, J. S.; Pichette, V.; Leblond, F.; Desbiens, K.; Beaulieu, P. Characterization of chronic constriction of the saphenous nerve, a model of neuropathic pain in mice showing rapid molecular and electrophysiological changes. *J. Neurosci. Res.* **2006**, *83*, 1310–1322.

(16) Merriam, F. V.; Wang, Z. Y.; Guerios, S. D.; Bjorling, D. E. Cannabinoid receptor 2 is increased in acutely and chronically inflamed bladder of rats. *Neurosci. Lett.* **2008**, 2008 Aug 31. [Epub ahead of print], doi:, 10.1016/j.neulet.2008.08.076.

(17) Iuvone, T.; De Filippis, D.; Di Spiezio Sardo, A.; D'Amico, A.; Simonetti, S.; Sparice, S.; Esposito, G.; Bifulco, G.; Insabato, L.; Nappi, C.; Guida, M. Selective CB2 up-regulation in women affected by endometrial inflammation. *J. Cell. Mol. Med.* **2008**, *12*, 661–670.

(18) Michalski, C. W.; Laukert, T.; Sauliunaite, D.; Pacher, P.; Bergmann, F.; Agarwal, N.; Su, Y.; Giese, T.; Giese, N. A.; Batkai, S.; Friess, H.; Kuner, R. Cannabinoids ameliorate pain and reduce disease pathology in cerulein-induced acute pancreatitis. *Gastroenterology* **2007**, *132*, 1968–1978.

(19) Benito, C.; Nunez, E.; Tolon, R. M.; Carrier, E. J.; Rabano, A.; Hillard, C. J.; Romero, J. Cannabinoid CB2 receptors and fatty acid amide hydrolase are selectively overexpressed in neuritic plaque-associated glia in Alzheimer's disease brains. *J. Neurosci.* **2003**, *23*, 11136–11141.

(20) Benito, C.; Tolon, R. M.; Pazos, M. R.; Nunez, E.; Castillo, A. I.; Romero, J. Cannabinoid CB2 receptors in human brain inflammation. *Br. J. Pharmacol.* **2008**, *153*, 277–285.

(21) Benito, C.; Kim, W. K.; Chavarria, I.; Hillard, C. J.; Mackie, K.; Tolon, R. M.; Williams, K.; Romero, J. A glial endogenous cannabinoid system is upregulated in the brains of macaques with simian immunodeficiency virus-induced encephalitis. *J. Neurosci.* **2005**, *25*, 2530–2536.

(22) Fernandez-Ruiz, J.; Romero, J.; Velasco, G.; Tolon, R. M.; Ramos, J. A.; Guzman, M. Cannabinoid CB2 receptor: a new target for controlling neural cell survival. *Trends Pharmacol. Sci.* **2007**, *28*, 39–45.

(23) Buckley, N. E.; McCoy, K. L.; Mezey, E.; Bonner, T.; Zimmer, A.; Felder, C. C.; Glass, M.; Zimmer, A. Immunomodulation by cannabinoids is absent in mice deficient for the cannabinoid CB2 receptor. *Eur. J. Pharmacol.* **2000**, *396*, 141–149.

(24) Muccioli, G.; Lambert, D. M. Latest advances in cannabinoid receptor antagonists. *Expert Opin. Ther. Pat.* **2006**, *16*, 1405–1423.

(25) Lunn, C. A.; Reich, E. P.; Fine, J. S.; Lavey, B.; Kozlowski, J. A.; Hipkin, R. W.; Lundell, D. J.; Bober, L. Biology and therapeutic potential of cannabinoid CB2 receptor inverse agonists. *Br. J. Pharmacol.* **2007**, *153*, 226–239.

(26) Giulio, G. M. Blocking the cannabinoid receptors: drug candidates and therapeutic promises. *Chem. Biodiversity* **2007**, *4*, 1805–1827.

(27) Rinaldi-Carmona, M.; Barth, F.; Millan, J.; Derocq, J.-M.; Casellas, P.; Congy, C.; Oustric, D.; Sarran, M.; Bouaboula, M.; Calandra, B.; Portier, M.; Shire, D.; Breliere, J.-C.; Fur, G. L. SR 144528, the first potent and selective antagonist of the CB2 cannabinoid receptor. *J. Pharmacol. Exp. Ther.* **1998**, *284*, 644–650.

(28) Lange, J. H.; Kruse, C. G. Keynote review: Medicinal chemistry strategies to CB1 cannabinoid receptor antagonists. *Drug Discovery Today* **2005**, *10*, 693–702.

(29) Ross, R. A.; Brockie, H. C.; Stevenson, L. A.; Murphy, V. L.; Templeton, F.; Makriyannis, A.; Pertwee, R. G. Agonist−inverse agonist characterization at CB1 and CB2 cannabinoid receptors of L759633, L759656, and AM630. *Br. J. Pharmacol.* **1999**, *126*, 665–672.

(30) Iwamura, H.; Suzuki, H.; Ueda, Y.; Kaya, T.; Inaba, T. In vitro and in vivo pharmacological characterization of JTE-907, a novel selective ligand for cannabinoid CB2 receptor. *J. Pharmacol. Exp. Ther.* **2001**, *296*, 420–425.

(31) Ueda, Y.; Miyagawa, N.; Wakitani, K. Involvement of cannabinoid CB2 receptors in the IgE-mediated triphasic cutaneous reaction in mice. *Life Sci.* **2007**, *80*, 414–419.

(32) Maekawa, T.; Nojima, H.; Kuraishi, Y.; Aisaka, K. The cannabinoid CB2 receptor inverse agonist JTE-907 suppresses spontaneous itch-associated responses of NC mice, a model of atopic dermatitis. *Eur. J. Pharmacol.* **2006**, *542*, 179–183.

(33) Ueda, Y.; Miyagawa, N.; Matsui, T.; Kaya, T.; Iwamura, H. Involvement of cannabinoid CB(2) receptor-mediated response and efficacy of cannabinoid CB(2) receptor inverse agonist, JTE-907, in cutaneous inflammation in mice. *Eur. J. Pharmacol.* **2005**, *520*, 164–171.

(34) Raitio, K. H.; Savinainen, J. R.; Vepsalainen, J.; Laitinen, J. T.; Poso, A.; Jarvinen, T.; Nevalainen, T. Synthesis and SAR Studies of 2-Oxoquinoline Derivatives as CB2 Receptor Inverse Agonists. *J. Med. Chem.* **2006**, *49*, 2022–2027.

(35) Shankar, B. B.; Lavey, B. J.; Zhou, G.; Spitler, J. A.; Tong, L.; Rizvi, R.; Yang, D. Y.; Wolin, R.; Kozlowski, J. A.; Shih, N. Y.; Wu, J.; Hipkin, R. W.; Gonsiorek, W.; Lunn, C. A. Triaryl bis-sulfones as cannabinoid-2 receptor ligands: SAR studies. *Bioorg. Med. Chem. Lett.* **2005**, *15*, 4417–4420.

(36) Lunn, C. A.; Fine, J. S.; Rojas-Triana, A.; Jackson, J. V.; Fan, X.; Kung, T. T.; Gonsiorek, W.; Schwarz, M. A.; Lavey, B.; Kozlowski, J. A.; Narula, S. K.; Lundell, D. J.; Hipkin, R. W.; Bober, L. A. A novel cannabinoid peripheral cannabinoid receptor-selective inverse agonist blocks leukocyte recruitment in vivo. *J. Pharmacol. Exp. Ther.* **2006**, *316*, 780–788.

(37) Page, D. S.; Brochu, M.-C.; Yang, H.; Brown, W.; St-Onge, S.; Martin, E.; Salois, D. Novel benzimidazole derivatives as selective CB2 inverse agonists. *Lett. Drug Des. Discovery* **2006**, *3*, 298–303.

(38) Diaz, P.; Xu, J. J.; Astruc-Diaz, F.; Pan, H.-M.; Brown, D. L.; Naguib, M. Design and synthesis of a novel series of *N*-alkyl isatin acylhydrazone derivatives that act as selective CB2 agonists for the treatment of neuropathic pain. *J. Med. Chem.* **2008**, *51*, 4932–4947.

(39) Pavlidis, V. H.; Perry, P. J. The Synthesis of a Novel Series of Substituted 2-Phenyl-4*H*-3,1-benzoxazin-4-ones. *Synth. Commun.* **1994**, *24*, 533–548.

(40) Quattropani, A.; Dorbais, J.; Covini, D.; Pittet, P. A.; Colovray, V.; Thomas, R. J.; Coxhead, R.; Halazy, S.; Scheer, A.; Missotten, M.; Ayala, G.; Bradshaw, C.; DeRaemy-Schenk, A. M.; Nichols, A.; Cirillo, R.; Tos, E. G.; Giachetti, C.; Golzio, L.; Marinelli, P.;

Church, D. J.; Barberis, C.; Chollet, A.; Schwarz, M. K. Discovery and Development of a New Class of Potent, Selective, Orally Active Oxytocin Receptor Antagonists. *J. Med. Chem.* **2005**, *48*, 7882–7905.

(41) Poso, A.; Huffman, J. W. Targeting the cannabinoid CB2 receptor: modelling and structural determinants of CB2 selective ligands. *Br. J. Pharmacol.* **2008**, *153*, 335–346.

(42) Stern, E.; Muccioli, G. G.; Bosier, B.; Hamtiaux, L.; Millet, R.; Poupaert, J. H.; Henichart, J. P.; Depreux, P.; Goossens, J. F.; Lambert, D. M. Pharmacomodulations around the 4-*oxo*-1,4-dihydroquinoline-3-carboxamides, a class of potent CB2-selective cannabinoid receptor ligands: consequences in receptor affinity and functionality. *J. Med. Chem.* **2007**, *50*, 5471–5484.

(43) Muccioli, G. G. Blocking the cannabinoid receptors: drug candidates and therapeutic promises. *Chem. Biodiversity* **2007**, *4*, 1805–1827.

(44) Raitio, K. H.; Savinainen, J. R.; Nevalainen, T.; Jarvinen, T.; Vepsalainen, J. Synthesis and in vitro evaluation of novel 2-*oxo*-1,2-dihydroquinoline CB2 receptor inverse agonists. *Chem. Biol. Drug Des.* **2006**, *68*, 334–340.

(45) Page, D.; Balaux, E.; Boisvert, L.; Liu, Z.; Milburn, C.; Tremblay, M.; Wei, Z.; Woo, S.; Luo, X.; Cheng, Y. X.; Yang, H.; Srivastava, S.; Zhou, F.; Brown, W.; Tomaszewski, M.; Walpole, C.; Hodzic, L.; St-Onge, S.; Godbout, C.; Salois, D.; Payza, K. Novel benzimidazole derivatives as selective CB2 agonists. *Bioorg. Med. Chem. Lett.* **2008**, *18*, 3695–3700.

(46) Gouldson, P.; Calandra, B.; Legoux, P.; Kerneis, A.; Rinaldi-Carmona, M.; Barth, F.; Le Fur, G.; Ferrara, P.; Shire, D. Mutational analysis and molecular modelling of the antagonist SR 144528 binding site on the human cannabinoid CB(2) receptor. *Eur. J. Pharmacol.* **2000**, *401*, 17–25.

(47) Montero, C.; Campillo, N. E.; Goya, P.; Paez, J. A. Homology models of the cannabinoid CB1 and CB2 receptors. A docking analysis study. *Eur. J. Med. Chem.* **2005**, *40*, 75–83.

(48) Tuccinardi, T.; Ferrarini, P. L.; Manera, C.; Ortore, G.; Saccomanni, G.; Martinelli, A. Cannabinoid CB2/CB1 selectivity. Receptor modeling and automated docking analysis. *J. Med. Chem.* **2006**, *49*, 984–994.

(49) Mukherjee, S.; Adams, M.; Whiteaker, K.; Daza, A.; Kage, K.; Cassar, S.; Meyer, M.; Yao, B. B. Species comparison and pharmacological characterization of rat and human CB2 cannabinoid receptors. *Eur. J. Pharmacol.* **2004**, *505*, 1–9.

(50) Kim, S. H.; Chung, J. M. An experimental model for peripheral neuropathy produced by segmental spinal nerve ligation in the rat. *Pain* **1992**, *50*, 355–363.

(51) Chaplan, S. R.; Bach, F. W.; Pogrel, J. W.; Chung, J. M.; Yaksh, T. L. Quantitative assessment of tactile allodynia in the rat paw. *J. Neurosci. Methods* **1994**, *53*, 55–63.

(52) Dixon, W. The up-and-down method for small samples. *J. Am. Stat. Assoc.* **1965**, *60*, 967–978.

(53) Cavasotto, C. N.; Orry, A. J.; Murgolo, N. J.; Czarniecki, M. F.; Kocsi, S. A.; Hawes, B. E.; O'Neill, K. A.; Hine, H.; Burton, M. S.; Voigt, J. H.; Abagyan, R. A.; Bayne, M. L.; Monsma, F. J., Jr. Discovery of novel chemotypes to a G-protein-coupled receptor through ligand-steered homology modeling and structure-based virtual screening. *J. Med. Chem.* **2008**, *51*, 581–588.

(54) Xie, X. Q.; Chen, J. Z.; Billings, E. M. 3D structural model of the G-protein-coupled cannabinoid CB2 receptor. *Proteins* **2003**, *53*, 307–319.

(55) Cherezov, V.; Rosenbaum, D. M.; Hanson, M. A.; Rasmussen, S. G.; Thian, F. S.; Kobilka, T. S.; Choi, H. J.; Kuhn, P.; Weis, W. I.; Kobilka, B. K.; Stevens, R. C. High-resolution crystal structure of an engineered human beta2-adrenergic G protein-coupled receptor. *Science* **2007**, *318*, 1258–1265.

(56) Rasmussen, S. G.; Choi, H. J.; Rosenbaum, D. M.; Kobilka, T. S.; Thian, F. S.; Edwards, P. C.; Burghammer, M.; Ratnala, V. R.; Sanishvili, R.; Fischetti, R. F.; Schertler, G. F.; Weis, W. I.; Kobilka, B. K. Crystal structure of the human beta2 adrenergic G-protein-coupled receptor. *Nature* **2007**, *450*, 383–387.

(57) Rosenbaum, D. M.; Cherezov, V.; Hanson, M. A.; Rasmussen, S. G.; Thian, F. S.; Kobilka, T. S.; Choi, H. J.; Yao, X. J.; Weis, W. I.; Stevens, R. C.; Kobilka, B. K. GPCR engineering yields high-resolution structural insights into beta2-adrenergic receptor function. *Science* **2007**, *318*, 1266–1273.

(58) Kobilka, B.; Schertler, G. F. New G-protein-coupled receptor crystal structures: insights and limitations. *Trends Pharmacol. Sci.* **2008**, *29*, 79–83.

(59) Ashton, J. C.; Wright, J. L.; McPartland, J. M.; Tyndall, J. D. Cannabinoid CB1 and CB2 receptor ligand specificity and the development of CB2-selective agonists. *Curr. Med. Chem.* **2008**, *15*, 1428–1443.

(60) Chen, J. Z.; Wang, J.; Xie, X. Q. GPCR structure-based virtual screening approach for CB2 antagonist search. *J. Chem. Inf. Model.* **2007**, *47*, 1626–1637.

(61) Cavasotto, C. N.; Abagyan, R. A. Protein flexibility in ligand docking and virtual screening to protein kinases. *J. Mol. Biol.* **2004**, *337*, 209–225.

(62) Cavasotto, C. N.; Kovacs, J. A.; Abagyan, R. A. Representing receptor flexibility in ligand docking through relevant normal modes. *J. Am. Chem. Soc.* **2005**, *127*, 9632–9640.

(63) Kovacs, J. A.; Cavasotto, C. N.; Abagyan, R. Conformational Sampling of Protein Flexibility in Generalized Coordinates: Application to Ligand Docking. *J. Comput. Theor. Nanosci.* **2005**, *2*, 354–361.

(64) Cavasotto, C. N.; Orry, A. J.; Abagyan, R. A. Structure-based identification of binding sites, native ligands and potential inhibitors for G-protein coupled receptors. *Proteins* **2003**, *51*, 423–433.

(65) Cavasotto, C. N.; Liu, G.; James, S. Y.; Hobbs, P. D.; Peterson, V. J.; Bhattacharya, A. A.; Kolluri, S. K.; Zhang, X. K.; Leid, M.; Abagyan, R.; Liddington, R. C.; Dawson, M. I. Determinants of retinoid X receptor transcriptional antagonism. *J. Med. Chem.* **2004**, *47*, 4360–4372.

(66) Monti, M. C.; Casapullo, A.; Cavasotto, C. N.; Napolitano, A.; Riccio, R. Scalaradial, a dialdehyde-containing marine metabolite that causes an unexpected noncovalent PLA2 Inactivation. *ChemBioChem* **2007**, *8*, 1585–1591.

(67) Xu, L.-Z.; Li, W.-H.; Song, H.-B.; Lia, K.; Yua, G.-P. (4-Chlorobenzoyl)methyl morpholine-4-carbodithionate. *Acta Crystallogr., Sect. E* **2005**, *61*, o130−o131.

(68) Brito, I.; Lopez-Rodriguez, M.; Cardenas, A.; Vargas, D. 4-(2,4-Dinitrophenylsulfanyl)morpholine. *Acta Crystallogr., Sect C: Cryst. Struct. Commun.* **2006**, *62*, o461−463.

(69) Otwinowski, Z.; Minor, W. Macromolecular Crystallography, Part A. In *Methods in Enzymology* Carter, C. W., Jr., Sweet, R. M., Eds.; Academic Press: San Diego, 1997; Vol. 276, pp 307−326.

(70) Altomare, A.; Burla, M. C.; Camalli, M.; Cascarano, G. L.; Giacovazzo, C.; Guagliardi, A.; Moliterni, A. G. G.; Polidori, G.; Spagna, R. SIR97: a new tool for crystal structure determination and refinement. *J. Appl. Crystallogr.* **1999**, *32*, 115–119.

(71) Sheldrick, G. M. *SHELXL97. Program for the Refinement of Crystal Structures*; University of Gottingen: Germany, 1994.

(72) Prince, E. International Tables for Crystallography. In *International Tables for Crystallography*; Hain, T., Ed.; Kluwer Academic Publishers: Dordrecht-Boston-London, 1992; Vol. C: Mathematical, Physical, and Chemical tables, pp255−578.

(73) Mirzadegan, T.; Benko, G.; Filipek, S.; Palczewski, K. Sequence analyses of G-protein-coupled receptors: similarities to rhodopsin. *Biochemistry* **2003**, *42*, 2759–2767.

(74) Ballesteros, J. A.; Weinstein, H.; Stuart, C. S. Integrated methods for the construction of three-dimensional models and computational probing of structure-function relations in G protein-coupled receptors. In *Methods in Neurosciences*: Academic Press: New York, 1995; Vol. 25, pp 366−428.

(75) Sali, A.; Blundell, T. L. Comparative protein modelling by satisfaction of spatial restraints. *J. Mol. Biol.* **1993**, *234*, 779–815.

(76) Zhang, R.; Hurst, D. P.; Barnett-Norris, J.; Reggio, P. H.; Song, Z. H. Cysteine 2.59(89) in the second transmembrane domain of human CB2 receptor is accessible within the ligand binding crevice: evidence for possible CB2 deviation from a rhodopsin template. *Mol. Pharmacol.* **2005**, *68*, 69–83.

(77) Johnson, M. R.; Melvin, L. S. *Cannabinoids as Therapeutic Agents*; CRC Press: Boca Raton, FL, 1986; pp 121−145.

JM801353P